

RESEARCH ARTICLE

Open Access

The pathogenic human Torsin A in *Drosophila* activates the unfolded protein response and increases susceptibility to oxidative stress

A-Young Kim^{1,2†}, Jong Bok Seo^{3†}, Won-tae Kim⁴, Hee Jeong Choi^{1,2}, Soo-Young Kim³, Genevieve Morrow⁵, Robert M Tanguay⁵, Hermann Steller⁶ and Young Ho Koh^{1,2*}

Abstract

Background: Dystonia1 (DYT1) dystonia is caused by a glutamic acid deletion (ΔE) mutation in the gene encoding Torsin A in humans (HTorA). To investigate the unknown molecular and cellular mechanisms underlying DYT1 dystonia, we performed an unbiased proteomic analysis.

Results: We found that the amount of proteins and transcripts of an Endoplasmic reticulum (ER) resident chaperone Heat shock protein cognate 3 (HSC3) and a mitochondria chaperone Heat Shock Protein 22 (HSP22) were significantly increased in the HTorA ^{ΔE} -expressing brains compared to the normal HTorA (HTorA^{WT}) expressing brains. The physiological consequences included an increased susceptibility to oxidative and ER stress compared to normal HTorA^{WT} flies. The alteration of transcripts of Inositol-requiring enzyme-1 (IRE1)-dependent spliced X box binding protein 1 (Xbp1), several ER chaperones, a nucleotide exchange factor, Autophagy related protein 8b (ATG8b) and components of the ER associated degradation (ERAD) pathway and increased expression of the Xbp1-enhanced Green Fluorescence Protein (eGFP) in HTorA ^{ΔE} brains strongly indicated the activation of the unfolded protein response (UPR). In addition, perturbed expression of the UPR sensors and inducers in the HTorA ^{ΔE} *Drosophila* brains resulted in a significantly reduced life span of the flies. Furthermore, the types and quantities of proteins present in the anti-HSC3 positive microsomes in the HTorA ^{ΔE} brains were different from those of the HTorA^{WT} brains.

Conclusion: Taken together, these data show that HTorA ^{ΔE} in *Drosophila* brains may activate the UPR and increase the expression of HSP22 to compensate for the toxic effects caused by HTorA ^{ΔE} in the brains.

Keywords: DYT1 dystonia, Bip, HSC3, HSP22, Xbp1

Background

The appearance of misfolded and aggregated proteins in specific regions of the brain is one of the common pathological hallmarks of various progressive neurological disorders in humans, such as early onset torsion dystonia (DYT1 dystonia) [1], Alzheimer's disease, Amyotrophic lateral sclerosis, Parkinson's disease, various polyglutamine diseases and prion disease [2]. A variety of evidence suggests that accumulated misfolded

proteins are key players in the onset and progression of these neurological disorders [1,2]. The endoplasmic reticulum (ER) is a sub-cellular organelle where secretory and membrane proteins are synthesised, modified, correctly folded and assembled prior to transit to the cell surface or to intracellular organelles. Perturbations of ER function, caused by various stressors, may result in the underlying deposition of intra- and/or extracellularly accumulated misfolded proteins in the brain, which has been associated with various neurological disorders [3,4]. The known ER stressors include physiological stress, pathological stress and environmental stress [5].

To sense and respond to ER stressors, eukaryotic cells have developed a group of evolutionarily conserved signal transduction pathways known as the unfolded

* Correspondence: kohyh@hallym.ac.kr

[†]Equal contributors

¹ILSONG Institute of Life Science, Hallym University, 1605-4 Gwanyangdong, Dongan-gu, Anyang, Gyeonggi-do 431-060, Republic of Korea

²Department of Biomedical Gerontology, Graduate School of Hallym

University, Chuncheon, Gangwon-do 200-702, Republic of Korea

Full list of author information is available at the end of the article

protein response (UPR), which is characterised by transcriptional up-regulation of ER resident chaperones, selective inhibition of translation, and activation of ER-associated degradation (ERAD) [6]. Under physiological conditions, the ER resident chaperone BiP, also known as Glucose-regulated protein 78 (GRP78), and Heat shock 70 kDa protein 5 (HSPA5) are bound to three UPR inducers, such as the pancreatic ER kinase (PERK), the inositol-requiring enzyme 1 (IRE1) and the activating transcription factor 6 (ATF-6). When unfolded proteins accumulate in the ER lumen, BiP binds to unfolded stretches in the proteins and becomes dissociated from the three UPR inducers, which subsequently activate the UPR that induces expression of BiP and other ER chaperones. If the increased BiP expression is sufficient for restoring ER function, it inactivates the UPR by binding to the three UPR inducers [4,6,7]. However, prolonged activation of the UPR by mild or strong ER stresses may result in the adaptation and survival of cells under these conditions or cell death [8]. Recent studies have shown that the prolonged activation of the UPR may contribute to the pathogenesis of autosomal dominant retinitis pigmentosa (ADRP) [9], Alzheimer's disease [10], Parkinson's disease [5,11], and Amyotrophic lateral sclerosis [12].

DYT1 dystonia is the most common and severe form of dystonia caused by mutations in the DYT1 gene encoding Torsin A in humans (HTorA). DYT1 patients show severe twisting movements and abnormal postures caused by involuntary muscle contractions. The loss of one of a pair of glutamic acid residues in HTorA (HTorA^{ΔE}) has been identified in most patients with this disorder [13]. Only 30-40% of heterozygous individuals manifest severe symptoms, suggesting that the ΔE mutation in HTorA may increase an individual's susceptibilities to other genetic and/or environmental risk factors required for the development of this disorder [14,15]. Amino acid sequence comparisons revealed that HTorA is a member of a family of ATPases associated with a variety of cellular activities (AAA+ATPase) and as such, may play a pivotal role in the assembly, disassembly, degradation and trafficking of other proteins [13,16]. Moreover, recent studies have shown that the secretory pathway in fibroblasts acquired from DYT1 dystonia patients is impaired [17], and the impaired secretory pathway in those cells is rescued by the down-regulation of HTorA^{ΔE} via the expression of an allele specific small interfering (si) RNA of HTorA^{ΔE} [18].

Another consequence of the ΔE mutation on HTorA at the subcellular level is the redistribution of HTorA^{ΔE} to the nuclear envelope (NE) that results in the appearance of perinuclear membranous inclusions in DYT1 dystonia fibroblasts [19], TorsinA^{ΔE} knock-in mouse brains [20], and transgenic mice over-expressing HTorA^{ΔE} in the brain [21]. At the molecular level, interactions between the HTorA^{WT} and its interaction partners, including the

Lamina-associated polypeptide 1 (LAP1) in the NE, the luminal domain like LAP1 (LULL1) in the ER [22,23], the NE network-associated protein Vimentin [24], and Kinesin light chain 1 (KLC1) [25,26] are abolished in the HTorA^{ΔE}. Recently, it has been shown that ultrastructural defects in the neuronal NE in the LAP1 knock out mouse are similar to those observed in the Tor1A^{ΔE} knock-in mouse, suggesting that HTorA and LAP1 may be present in the same signal transduction pathway that regulates normal development of the neuronal NE [26]. These reports suggest that DYT1 pathogenesis could be the consequence of altered transcriptional regulation caused by abnormal interactions of HTorA^{ΔE} with nuclear envelope proteins and/or a loss of function of HTorA^{WT} in the ER that would impair certain neuron-specific signalling pathways.

To investigate how transcriptional or translational alterations contribute to the pathogenesis of DYT1, unbiased genomics and proteomic analyses were recently performed using *in vitro* and *in vivo* DYT1 models. The expression of HTorA^{ΔE} in neuronal cell lines did not induce transcriptional alterations; however, expression changes of proteins involved with energy metabolism and the redox state were detected in this model [27]. A recent study revealed that the expression of several genes involved in the development and function of the nervous system, cytoskeleton organisation and biogenesis, cell adhesion, G-protein-receptor signalling and the vesicle mediated trafficking pathway were altered when transcriptional profiles in peripheral blood cells from DYT1 dystonia patients were compared with those of HTorA^{ΔE} carriers [28].

Drosophila has been extensively utilised as a model to investigate the molecular and cellular aetiologies underlying diverse neurological diseases in humans. We have shown that HTorA^{ΔE} but not HTorA^{WT} expressed in *Drosophila* induced protein aggregates near the NE, caused defects at synaptic terminals, and increased the flies' susceptibility to environmental stress [29,30]. In this study, we gained further insights into the molecular and cellular consequences of HTorA^{ΔE} in *Drosophila* brains by performing an unbiased 2-dimensional electrophoresis analysis that demonstrated that Heat shock protein cognate 3 and Heat shock protein 22 were dysregulated with the expression of HTorA^{ΔE}. In addition, we performed biochemical, behavioural, cellular and molecular biological, genetic, pharmacological and proteomics profiling analyses to provide several lines of evidence supporting the observation that UPR activation and increased susceptibility to oxidative stress were the consequences of HTorA^{ΔE} expression in *Drosophila*.

Methods

Fly genetics

UAS-HTorA^{WT}, UAS-HTorA^{ΔE}, Tubulin-Gal4, C155-Gal4 [29,30], *xbp1*^{K13803}/CyO and UAS-Xbp1-eGFP [31] were

previously characterised. Tubulin-Gal4, UAS-HTorA^{WT}/TM6b Tb¹ and UAS-HTorA^{ΔE}/CyO, P{GAL4-Kr.C}DC3, P{UAS-GFP.S65T}DC7 flies were generated via chromosome recombination. RNAi flies for Xbp1, HSC3, Activation transcription factor 6 (ATF6) and Pancreatic eIF-2a kinase (PEK) and *X box binding protein -1(xbp1)*^{K13803}/CyO were obtained from the Vienna *Drosophila* RNAi Center (VDRC) and the Bloomington stock centre. UAS-Actin-GFP (Act-eGFP) flies were obtained from Bloomington stock centre. UAS-DTor-cDNA (DTor) flies were generated by cloning full length DTor-cDNA into pUAST germ line transformation vectors. Flies were reared on a standard *Drosophila* medium in a 16 h light – 8 h dark cycle at 25 ± 1°C and 60 ± 1% relative humidity.

2-Dimensional electrophoresis

As described in Koh et al. [29], Tubulin-Gal4/UAS-HTorA^{WT} and UAS-HTorA^{ΔE/+}; Tubulin-Gal4/+ flies collected from three different independent crosses were raised at 30°C for accelerating aging. Proteins were extracted from 10 day old adult fly heads by grinding for 5 min using a manual pestle in 100 μL lysis buffer (8.0 M urea, 18 mM DTT, 4% (w/v) CHAPS, 40 mM Tris-HCl (pH 8.0), 10 mM EDTA, 0.5% IPG buffer (pH4-7, GE healthcare, Germany) with protease inhibitor cocktail (Roche Diagnostics, GmbH, Germany). Next, 300 μL of lysis buffer was added, the solution was centrifuged at 15,000 rpm (Vision scientific Co., Korea) for 10 min and the supernatants were collected. The concentrations of proteins were quantified using the Bradford assay. A total of 200 μg of proteins were applied on immobilised linear gradient strips (pH 4–7) using the IPGphor system (Amersham Pharmacia Biotech, Uppsala, Sweden). After rehydration for 12 hr, focusing was performed in the following three steps: 200 V for 1 hr, 500 V for 1 hr and a final phase of 8,000 V for 8 hr. After the reduction and alkylation, proteins were achieved by incubating strips for 15 min while shaking in 1.5 M Tris-HCl buffer (pH 8.8, 10% SDS, 87% glycerol, 6 M urea, 64.8 mM DTT), and the second dimension was run on a 12% poly-acrylamide SDS gel using an Ethan Dalt electrophoresis kit (Amersham Pharmacia Biotech., Uppsala, Sweden). Two-D gels stained with 0.1% Coomassie Brilliant Blue R250 were scanned with a PowerLook III image scanner (UMAX data system, Hsinchu, Taiwan) and analysed using Progenesis Editor software (Nonlinear Dynamics Ltd., Newcastle, UK) with the exclusion filter set manually. The total number of protein spots on the 6 gels ranged from 1415 to 2534 (WT1, 1415; WT2, 1927; WT3, 2534; ΔE1, 1444, ΔE2, 1928, and ΔE3, 2178). The normalised volumes of the protein spots from three different comparisons were analysed using one-way Anova (threshold of significance; P < 0.05) to select protein spots for subsequent analyses.

Identification of proteins in differentially expressed protein spots

Seven differentially expressed spots were excised from the gels, washed with 10 mM NH₄HCO₃ and 50% CH₃CN (Sigma), and digested in a buffer containing 50 mM NH₄HCO₃, 5 mM CaCl₂, and 12.5 ng/ml Trypsin Gold (Promega, Madison, WI, USA) at 37°C for 12–16 h. The digested peptides were recovered by extraction twice with 50 mM NH₄HCO₃ and 100% CH₃CN. The resulting peptide extracts were pooled, lyophilised in a vacuum centrifuge and stored at 4°C for subsequent protein identification. The protocol for protein identification was published by Lee et al. [32]. A nano LC/MS system consisting of a Surveyor HPLC system (Thermo Scientific, Waltham, MA, USA) and ESI-quadruple IT MS (LCQ Deca XP-Plus, Thermo Scientific, Waltham, MA) equipped with a nano-ESI source was used to perform the MS/MS experiments for protein identification. For desalting and concentration, 10 μl of digested sample was loaded by the auto sampler onto a C18 trap column (I.D 300 μm, length 5 mm, particle size 5 μm; DIONEX/LC Packings, Sunnyvale, CA) at a flow rate of 20 μl/min. To separate trapped peptides, the samples were back-flushed into a home-made microcapillary column (150 mm in length) packed with C18 resin (particle size 5 μm) in 75-μm silica tubing (8-μm id orifice) using mobile phases, A and B, composed of 0% and 80% of CH₃CN containing 0.02% HCO₂H and 0.5% CH₃COOH, respectively.

The gradient initiated with 5% of the mobile phase B and 95% of the mobile phase A for 15 min. The mobile phase B was increased from 20% for 3 min, to 50% for 32 min, to 60% for 5 min, to 80% for 5 min, to 100% for 2 min and finally held at 100% for 8 min. The column was equilibrated and cleaned with 5% CH₃CN for 10 min between running samples. The operating conditions for obtaining MS and MS/MS spectra were as follows: a capillary temperature of 220°C, an ESI voltage of 2.5 kV, and a collision energy setting at 35%. The three most abundant MS ions from MS were selected as peaks. Mass spectrometric analysis was included with the MS/MS analysis of the three most abundant ions from MS and 180 second dynamic exclusion. The Xcalibur data system (Thermo Finnigan, USA) was used to control MS scan functions and HPLC solvent gradients. MS/MS spectra were searched against the proteins extracted with *Drosophila* from a non-redundant protein database at NCBI (<ftp://ftp.ncbi.nlm.nih.gov/blast/db/FASTA/>) using the SEQUEST (version 3.3.1, Thermo, USA) searching algorithm from the Bioworks (version 3.3.1, Thermo, USA) software package with the following parameters: a mass tolerance of 2.0 Da on the parent ion and 1.0 Da on the MS/MS, one missed cleavage per peptide allowed, and modifications of proteins were not considered. Mass peak lists were analysed for the

b and *y* ions. The search results were filtered using the cross-correlation score (X_{Corr}) and the normalised difference in cross-correlation scores (ΔC_n). Matched peptide sequences had to pass the following thresholds: 1) the uniqueness scores of matches (ΔC_n) were at least 0.1 and 2) minimum cross-correlation scores X_{Corr} of 1.9, 2.2, and 3.75 for charge states +1, +2, and +3, respectively. The search results were saved automatically. An SRF file including the merging of proteins, filter and sort settings, ratios and protein area/height values was used to select and sort peptide/spectrum matches passing this set of criteria. Proteins were identified using more than two peptides per spot.

Anti-HSC3 western blot analysis

Ten adult fly heads were homogenised in ice-cold radio-immuno-precipitation assay (RIPA) buffer (150 mM NaCl, 1% IGEPAL CA-630, 0.5% Na-oxcholate, 0.1% SDS, 50 mM Tris, pH 8.0; Sigma-Aldrich, St. Louis, MO) with protease inhibitors (Halt™ protease inhibitor cocktail, Thermo Fisher Scientific, Rockford, IL). The homogenate was centrifuged at 14,000 *g* for 20 minutes at 4°C to remove cellular debris. The quantification of proteins in supernatants was accomplished using the BCA protein assay kit (Thermo Fisher Scientific).

For western blot analysis, 20.0 µg of total protein from each sample was separated on an 10% tri-glycine polyacrylamide SDS gel and then transferred to a nitrocellulose membrane (GE Healthcare Bio-Sciences AB, Uppsala, Sweden). The membranes were probed with rat-anti-HSC3 antibody (1:5,000; Babraham Bioscience Technologies Limited, Cambridge, UK) [32] and mouse monoclonal anti- α -tubulin antibody (1:2,000; Developmental Studies Hybridoma Bank, University of Iowa, Iowa City, IA) and were developed using the peroxidase-conjugated goat anti-rat IgG or goat anti-mouse-IgG (Thermo Fisher Scientific) and Supersignal West Pico (Thermo Fisher Scientific). The intensities of the bands were semi-automatically quantified using a wand tool and a histogram function in the Adobe Photoshop program (Adobe, San Jose, CA), as previously published [33]. Statistical analyses were performed with the Minitab software (Minitab Inc., State College, CA).

Anti-HSP22 western blot analysis

HSP22 is a mitochondria resident chaperone [34]. The crude mitochondria pellet preparation method was modified from Miwa et al. [35] and Morrow et al. [36]. Briefly, flies were either not heat shocked or heat-shocked for 30 min at 37°C and allowed to recover for 4 hours at RT. Fly heads were grinded in 300 µl of ice-cold mitochondria homogenisation buffer (pH 7.4, 280 mM sucrose, 10 mM HEPES, 1 mM EDTA; Sigma-Aldrich) with protease inhibitors (Halt™ protease inhibitor cocktail, Thermo-Fisher

Scientific). The homogenate was centrifuged at 750 *g* for 10 min at 4°C to remove cellular debris. To pellet crude mitochondria, the supernatant was centrifuged at 17,000 *g* for 10 min at 4°C. The pellet was re-suspended in 100 µl of ice-cold mitochondria homogenisation buffer. The BCA assay was then performed for protein quantification. A total of 2.98 µg of crude mitochondria samples was separated using 12% SDS-PAGE and then transferred to nitrocellulose membranes. The blots were probed with rabbit anti-HSP22 (1:5,000) [34] and developed with the peroxidase-conjugated goat anti-rabbit IgG (Thermo Fisher Scientific) and Supersignal West Pico (Thermo Fisher Scientific). Quantification and statistical analyses of band intensities were performed as described above.

Anti-DTor antibody production and western blot analysis

His-tagged DTor recombinant peptides (residue 25–200) expressed in *Escherichia coli* M15 (Qiagen) were purified using Ni-NTA beads (Qiagen). After separated by SDS-PAGE, peptides were injected into rabbits for polyclonal antibody production.

Proteins were extracted from Tub-Gal4/+ and UAS-DTor/+;Tub-Gal4/+ larval body wall muscle preparation. After separated by a 10% SDS-PAGE, proteins were transferred to a nitrocellulose membrane (GE Healthcare Bio-Sciences AB). The membranes was probed with rat-anti-HSC3 antibody (1:5,000; Babraham Bioscience Technologies Limited) [32], mouse monoclonal anti- α -tubulin antibody (1:2,000; Developmental Studies Hybridoma Bank) and rabbit-anti-DTor antibodies (1:10,000) and were developed using the peroxidase-conjugated goat anti-rat IgG, goat anti-mouse-IgG, and goat anti-Rabbit-IgG (Thermo Fisher Scientific) and Supersignal West Pico (Thermo Fisher Scientific). Quantification and statistical analyses of band intensities were performed as described above.

Quantitative real time PCR (qRT-PCR)

Total RNA was extracted from 30 heads of adult flies using Trizol® reagent (Invitrogen, Carlsbad, CA). The purity and integrity of the total RNA were determined according to the A_{260}/A_{280} ratio and 28S rRNA/18S rRNA ratio, respectively. The A_{260}/A_{280} ratio of the RNA samples used in this study was above 1.6, and the rRNA 28S/16S ratio was approximately 2:1 (data not shown). After treating with DNase I (Promega, Madison, WI), complementary DNA (cDNA) was synthesised from 4 µg of total RNA using cDNA synthesis kits (Invitrogen). Quantitative real-time (qRT) PCR analysis was performed on a 7300 Real-Time PCR System (Applied Biosystems, Foster City, CA) using SYBR® Green PCR Master Mix (Applied Biosystems). The PCR conditions were 95°C for 10 min, followed by 40 cycles of 95°C for 15 s, 60°C for 20 s, and 72°C for 30 s for all target genes. The specificity of primer

pairs (Additional file 1) used in this study was determined via dissociation curves and sequencing of amplified PCR fragments (data not shown). The PCR amplification efficiency of each primer pair was established using calibration curves (Additional file 2). Correlation coefficients (r^2) and the slopes were >0.98 and between -3.114 and -3.654 , respectively, for all experiments (Additional file 2). The PCR efficiencies calculated for each primer pair using the equation $= 10^{-1/\text{slope}} - 1$ [37] were from 0.90126 to 1.09436 for all experiments (Additional file 2). Relative mRNA levels were adjusted with the internal control RP49 and calculated using the $2^{-\Delta\Delta\text{CT}}$ method [37]. All reactions were performed in duplicate technically and in triplicate biologically.

Anti-enhanced Green fluorescence Protein (eGFP) Western blot analysis

To examine the UPR activation *in vivo*, 10 day old adult brains of UAS-Xbp1-eGFP/Tub-Gal4, UAS-HTorA^{WT} and UAS-HTorA^{ΔE} /+;Tub-Gal4/UAS-Xbp1-eGFP were homogenised in RIPA buffer. A total of 15 μg of head protein extracts was separated using 10% SDS PAGE. Rabbit polyclonal anti-GFP antibody (sc-8334, Santa Cruz Biotechnology, Inc., Santa Cruz, CA) was used to detect the amount of Xbp1-eGFP. Anti-α-Tubulin antibody (DSHB) was used as a loading control. Quantification and statistical analyses of band intensities were performed as described above.

Oxidative and ER stress sensitivity assay

To investigate the changes in oxidative and ER stress in *Drosophila*, a modified version of the oxidative and ER stress protocol from Meulener et al. [38] and Park et al. [33] was used. Briefly, each group of flies consisted of 5 males and 5 females that were 10 days old, which were transferred into a vial containing 1% agar, 5% sucrose with 20 mM paraquat (Sigma-Aldrich) or 1% H₂O₂ (Merck KGaA, Darmstadt, Germany) and kept at $25 \pm 1^\circ\text{C}$ and $60 \pm 1\%$ relative humidity. To induce ER stress, each group of flies was transferred to a vial containing 1% agar, 5% sucrose with 12 μM tunicamycin (Santa Cruz biotechnology, inc. Santa Cruz, CA), and 5 mM, 25 mM, or 100 mM dithiothreitol (DTT; Invitrogen, Carlsbad, CA). Flies were transferred to newly prepared tubes every other day. The number of dead flies was counted every 12 hours until 120 hours. Ten-independent tests were performed for each genotype. Two-sample t-tests were performed using Minitab software (Minitab). When the flies were treated with only 1% agar and 5% sucrose, there were no differences in survival rates between the HTorA^{WT}- and HTorA^{ΔE}-expressing flies (Additional file 3). A Kaplan-Meier survival analysis was performed using R (version 3.0.1. The R foundation for Statistical Computing) software.

Autophagy inhibitor treatments

To inhibit autophagy, each group of flies consisting of 5 males and 5 females that were 10 days old were transferred into a vial containing 1% agar, 5% sucrose with 10 mM 3-methyladenine (3-MA;Sigma-Aldrich), 40 μM wortmanin (LC laboratory, Woburn, MA), and 40 μM LY294002 (LC laboratory) and kept at $25 \pm 1^\circ\text{C}$ and $60 \pm 1\%$ relative humidity as described previously [33]. The flies were transferred to newly prepared tubes every other day. The number of dead flies was counted every 12 hours. Ten-independent tests were performed for each genotype. A Kaplan-Meier survival analysis was performed using R (version 3.0.1. The R foundation for Statistical Computing) software.

Density gradient sub-cellular fractionation

To obtain microsomes derived from endoplasmic reticulum in *Drosophila* brains, a modified version of the density gradient sub-cellular fractionation protocol from Xia et al. [39] and Tan et al. [40] was used. Briefly, one hundred adult fly heads were grinded and placed in 390 μl ice-cold isotonic homogenisation medium (0.25 M sucrose, 5 mM EDTA, 10 mM Tris-HCl, 50 mM KCl, pH7.5; Sigma-Aldrich) containing protease inhibitors (Halt™ protease inhibitor cocktail, Thermo-Fisher Scientific). The homogenate was centrifuged at 3000 g for 10 min at 4°C to remove cellular debris and nuclei. The amounts of proteins in the supernatants were measured using the BCA method, and equal amounts of proteins were used for further separations. The supernatant was then centrifuged in a S120AT2 rotor at 100,000 g for 1 hr at 4°C using a Himac CS 120EX (Hitachi, Japan). The resultant vesicle pellets were re-suspended in 1 ml of membrane suspension buffer (0.25 M sucrose, 50 mM KCl, 5 mM EDTA, 10 mM Tris-HCl, pH7.5; Sigma-Aldrich). Discontinuous Iodixanol gradients were generated using 60% Iodixanol (OptiPrep™, Axis-Shield PoC AS, Oslo, Norway) with dilution buffer (300 mM KCl, 30 mM EDTA, 60 mM Tris-HCl, pH 7.5) and set up in ultracentrifuge tubes as follows: 40% Iodixanol, 100 μl; 35% Iodixanol, 150 μl; 30% Iodixanol, 200 μl; 25% Iodixanol, 350 μl; 20% Iodixanol, 500 μl; 10% Iodixanol, 450 μl; 5% Iodixanol, 250 μl; 2.5% Iodixanol, 100 μl). The re-suspended vesicle fractions were loaded on top of the gradients and centrifuged in a S100AT5 rotor at 340,000 g for 3 hr at 4°C using a Himac CS 120EX (Hitachi, Japan). The resulting gradient was harvested in 200 μl fractions. Ten μl from 12 fractions was separated using 8% SDS-PAGE and then transferred to nitrocellulose membranes. To identify ER fractions, the membranes were blotted with rat anti-HSC3 antibodies as described above.

Protein extraction, SDS-PAGE and In-Gel digestion

One hundred μL of density gradient solutions from fraction Nos. 9 to 12 was boiled with SDS sample buffer for 10 min and concentrated using Vivaspin 500 (3,000 M.W. cut off; Satorius AG, Goettingen, Germany) before loading onto 10% SDS PAGE gels. The gels were stained with Coomassie brilliant blue. Each lane was split into 5 pieces that were digested individually with Trypsin-Gold (Promega) as described above. After incubation, digested peptides were extracted using an Oasis HLB extraction cartridge with C18 resin (Waters, MA, USA). Peptides in aqueous solution were loaded onto the columns washed with 0.5% Acetic acid/5% CH_3CN and eluted in 0.5% Acetic acid/100% CH_3CN . The peptide extracts were lyophilised in a vacuum centrifuge and stored at 4°C for subsequent identification and semi-quantification of proteins.

Identification and semi-quantification of proteins present in HSC3 positive density gradient fractions using label-free proteomics

Previously published label-free proteomic methods [41,42] were modified and used. Lyophilised peptides were resuspended in 20 μL of 0.1% formic acid with 50 fmol/ μL of MassPrep yeast enolase digestion standard (Waters) prior to LC/MS^E analysis. Each sample was analysed in three independent experimental runs with LC/MS^E using a nanoACQUITY ultra pressure liquid chromatography (UPLC) and a Synapt Q-Time of Flight (TOF) mass spectrometer equipped with a Nanolockspray ion source (Waters, Manchester, UK). A Mass PREP Digestion Standard (Protein Expression Mixture 1 & 2) (Waters) was run before and after the samples to monitor sensitivity and quantity. Two μL of sample was injected online onto a Waters Symmetry C18 trapping column (180 μm i.d. X 20 mm length with 5 μm particle size) at a flow rate of 10 $\mu\text{L}/\text{min}$ in 0.1% formic acid for 5 min. Peptides were eluted off the precolumn and separated by inline gradient elution onto a 75 μm i.d. X 200 mm length column packed with BEH130 C18 resin, 1.7 μm particle size, at a flow rate of 300 nL/min using a linear gradient from 3 to 45% B over 55 min (A; 0.1% formic acid in water, B; 0.1% formic acid in acetonitrile), followed by 25 min rinses at 90% B. The column was re-equilibrated with 3% B for 20 minutes prior to the next run. All column temperatures were maintained at 35°C . The mass accuracy was maintained during the run using Nanolockspray of the peptide [glu1]-fibrinopeptide B delivered through the auxiliary pump of NanoACQUITY at a concentration of 400 fmol/ μL and a flow rate of 500 nL/min. The peptides were analysed in positive ion mode and were operated in v-mode with a typical resolving power of 10,000 fwhm. Prior to the analyses, the TOF analyser was calibrated using [glu1]-fibrinopeptide B fragments that were obtained using a collision energy of 30 eV and over the

mass range 50–1990 m/z. The Q-TOF was operated in the LC/MS^E mode of acquisition. The MS^E mode was programmed to acquire data with a proprietary dual exact mass protocol. The two acquisition functions were rapidly alternated between low and elevated collision energies. One second scans of low and elevated high collision energy resulted in the acquisition of a time-resolved global protein expression dataset containing two data functions; the first was composed exclusively of conventional, low energy MS spectra (intact peptide ions), and the second was composed of mass spectra acquired at an elevated high collision energy (peptide product ions). Low energy data collections were performed at a constant collision energy of 4 eV, and high collision energy acquisitions were performed using a 15–40 eV ramping. The [glu1]-fibrinopeptide at a concentration of 400 fmol/ μL (m/z 785.8426) was infused via the nanolockspray ion source at a flow rate of 500 nL/min and sampled every 30 s as an external mass calibrant. For each injection, the mass spectrometer acquired data from 0 to 90 min. The Water Protein Expression System Informatics incorporated in ProteinLynx Global SERVER version 2.4 (PLGS 2.4) was used to process all raw data files. Each processed file was then searched against the *Drosophila melanogaster* protein database obtained from UniProt (<http://www.uniprot.org/uniprot/?query=taxonomy:7227>) with *Saccharomyces cerevisiae* enolase (P00924) appended. Protein identifications from the low/high collision spectra for each sample were processed using a hierarchical approach where detection of at least 3 fragment ion matches per peptide, 7 fragment ion matches per protein and 2 peptide matches per protein were required. The fixed and variable modifications considered were carbamidomethylation of cysteine residues and oxidation of methionine, respectively, with one allowable missed cleavage. All proteins identified with high confidence and with more than two peptides were considered for protein quantification. In relative protein quantitative analyses, multiple normalised global expression datasets were compared and contrasted. Exact mass retention time (EMRT) signatures enabled all detected proteins to be uniquely identified. The EMRT signatures of any two global expression datasets to be compared were matched. The normalised intensity of each EMRT signature was indicative of the abundance of a specific tryptic peptide. Each protein in a global expression dataset was represented by multiple peptides, so the relative quantitation of any protein was calculated by comparing an average and relative protein fold-change of multiple matched EMRT signatures. We considered significantly regulated proteins with a likelihood of quantification smaller than 0.05. The entire data set of differentially expressed proteins was further filtered by considering the identified peptides that replicated two out of three technical instrument replicates with an over 80 protein

probability score (Additional file 4). The label-free semi-quantification results of density gradient fractions were summarised in Additional file 5.

Life span analysis of the HTorA^{ΔE} flies with down-regulated UPR sensors and inducers in the neuronal system

The expression of *hsc3*, *xbp1*, *ATF6* and *PEK* in the neuronal systems of the flies was down-regulated by crossing RNAi construct flies with pan-neuronal Gal4 drivers, C155-Gal4. The levels of transcripts of each gene down-regulated by its RNAi flies were confirmed using qRT-PCR (Additional file 6). Among 3 lines of the *hsc3*-RNAi flies tested, only one line that gave rise to the adult flies when crossed with C155-Gal4 driver flies was used to test the consequences of down-regulated *hsc3* at the neuronal systems with (C155/+;*hsc3*-RNAi/+) or without HTorA^{ΔE} (C155/+;UAS-HTorA^{ΔE}/*hsc3*-RNAi). The *xbp1*-RNAi and the *xbp1*^{K13803}/CyO flies previously characterised [43] were used in this study to examine the consequences of a reduced amount of *xbp1* in fly brains with or without HTorA^{ΔE}. The *ATF6*-RNAi and the *PEK*-RNAi flies were crossed with the pan-neuronal Gal4 flies with or without HTorA^{ΔE}-expression, and then the consequences were examined. The numbers of live flies in 12 ~ 15 vials of each genotype were counted every 3 ~ 4 days. Only female flies raised at 25°C were used for this analysis. A Kaplan-Meier survival analysis was performed using R (version 3.0.1. The R foundation for Statistical Computing) software.

Results

Six proteins in 7 spots were differentially expressed in HTorA^{ΔE}-expressing fly brains

Figure 1A shows representative 2-dimensional electrophoresis (DE) images of soluble proteins extracted from adult fly brains expressing human TorsinA (HTorA)^{WT} and HTorA^{ΔE}. The normalised volumes of spot 302, 306, 309, 853 and 1783 were significantly increased in the HTorA^{ΔE}-expressing brains, whereas the normalised volumes of spots 640 and 775 were significantly decreased in the HTorA^{ΔE}-expressing brains (Figure 1). Even though proteins in spots 302, 306 and 309 had different isoelectric points, similar size-dependent migration patterns suggested that the major proteins in these spots might have been the same proteins with different post-transcriptional modifications (Figure 1B and C). Indeed, Heat shock protein cognate 70-3 (HSC3) was commonly identified in spots 302, 306, and 309 (Figure 1C, Table 1, and Additional file 7). In addition, Transferrin 1 (Tsf1) was identified in spots 302 and 309 (Figure 1B, Table 1, and Additional file 7). Cuticular protein 72Ec (Cpr72), lethal (2) 37Cc, Sarcoplasmic calcium binding protein 1 (Scp1), and Heat shock protein 22 (HSP22) were identified

in spots 640, 775, 853, and 1783, respectively (Table 1, Additional file 7).

Significantly increased HSC3 and HSP22 proteins in HTorA^{ΔE}-expressing brains

HTorA belongs to the AAA+ ATPase family and localises to the lumen of the endoplasmic reticulum (ER) [16]. The consequence of a ΔE mutation in HTorA was a preferential localisation of the HTorA aggregates at the nuclear envelope (NE) and in the ER in diverse animal and cellular models [29,44,45]. We further verified the increased expression of HSC3 and HSP22 in the HTorA^{ΔE}-expressing brains compared to the HTorA^{WT}-expressing brains by performing western blot analysis using rat anti-HSC3 and rabbit anti-HSP22 antibodies. The HSC3 proteins in the HTorA^{ΔE}-expressing brains were increased 1.4-fold compared to the levels expressed in the HTorA^{WT}-expressing brains. However, HSC3 proteins in Act-eGFP expressing brains were similar to those of HTorA^{WT}-expressing brains (Figure 2A and B). We also further tested whether expression of *Drosophila* Torsin (DTor) induced any change in HSC3 expression. Even DTor proteins in DTor overexpressing brains were increased 3.5-fold compared to the levels of Tub-Gal4/+ control flies, there was no change in HSC3 expression (Additional file 8). In addition, HSP22 proteins were detected from only the HTorA^{ΔE} flies in normal condition (Figure 2C), and a 3.4-fold increase of HSP22 was observed in the HTorA^{ΔE}-expressing brains compared to the HTorA^{WT}-expressing brains following heat shock (Figure 2C and D). These data confirmed that the amount of HSC3 and HSP22 were increased in the HTorA^{ΔE}-expressing brains.

Transcripts of HSC3 and HSP22 were increased in HTorA^{ΔE}-expressing brains

On the basis of the proteomic results for *hsc3* and *hsp22*, we next checked their transcript levels compared to those of controls by performing quantitative real-time PCR (qRT-PCR). The transcripts of *hsc3*, *tsf1* and *hsp22* in the HTorA^{ΔE}-expressing fly brains were significantly higher than those in the HTorA^{WT}-expressing fly brains, but there was no difference in transcript levels of *scp1* between the HTorA^{WT}- and the HTorA^{ΔE}-expressing brains (Figure 3A and B). Because *hsc3* has two very closely related genes (*hsc4* and *hsc5*) in the fly genome, we confirmed that there were no differences in the levels of expression of *hsc4* and *hsc5* transcripts between the HTorA^{WT}- or the HTorA^{ΔE}-expressing brains.

Increased IRE1-dependent spliced x-box binding protein 1 (*xbp1*) mRNA in the HTorA^{ΔE}-expressing brains

Previous studies have shown that the transcripts of *hsc3* and *hsp22* are increased when flies are exposed to ER

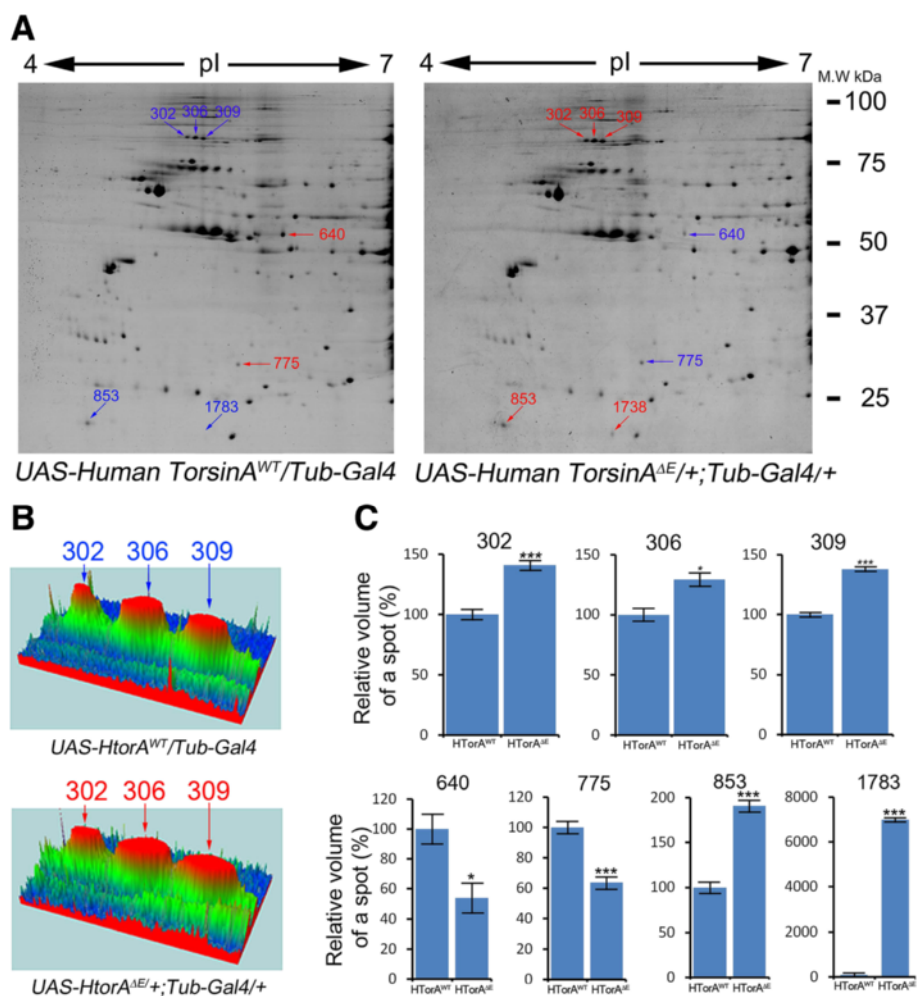


Figure 1 A representative comparison of protein expression patterns between fly brains expressing HtorA^{WT} and HtorA^{ΔE} using 2-DE. **(A)** Differentially expressed protein spots of the HtorA^{WT}- and the HtorA^{ΔE}-expressing flies were labeled with Coomassie brilliant blue staining. Blue colors indicate lower amounts of proteins, and red colors represent significantly more proteins. **(B)** Representative 3D-views of 3 differentially expressed spots. **(C)** Quantification results of differentially expressed spots. * = $p < 0.05$, *** = $p < 0.001$.

stress that activates the UPR [31] and oxidative stress [46], respectively. To determine whether the UPR in the HtorA^{ΔE}-expressing flies was induced, the levels of unspliced and IRE1-dependent spliced forms of x-box binding protein 1 (*xbp1*) mRNA were examined using performing qRT-PCR. Previous studies in *Drosophila* have shown that the levels of an IRE1-dependent spliced form of *xbp1* mRNA are increased upon activation of the UPR [31,47]. The levels of unspliced *xbp1* mRNA were similar between the HtorA^{WT}- and the HtorA^{ΔE}-expressing brains. In contrast, the level of spliced *xbp1* mRNA was significantly increased in the HtorA^{ΔE}-expressing brains compared with those of the HtorA^{WT}-expressing flies (Figure 3C). These results suggest that HtorA^{ΔE} initiates the UPR in the ER.

To further confirm that the IRE1-dependent splicing of *xbp1* mRNA was induced by HtorA^{ΔE}, we used a

xbp1-eGFP reporter that allowed eGFP to be expressed only when a 23 bp intron was spliced out of the *xbp1*-eGFP construct by IRE1 in the ER [31]. Compared with protein extracts of the brains of the control flies (UAS-*xbp1*-eGFP/Tub-Gal4, UAS-HtorA^{WT}), the brains of the HtorA^{ΔE}-expressing flies (UAS-HtorA^{ΔE/+}; Tub-Gal4/UAS-*xbp1*-eGFP) showed significantly increased amounts of Xbp1-eGFP signals that were detected using anti-GFP antibodies (Figure 3D and E). These results show that HtorA^{ΔE} activates the UPR through IRE1-dependent splicing of Xbp1 mRNA.

Increased oxidative and ER stresses in the HtorA^{ΔE}-expressing flies

The altered transcription and protein expression of HSC3 and HSP22 in the HtorA^{ΔE}-expressing fly brains suggested that the HtorA^{ΔE}-expressing flies might have

Table 1 Summary of identified proteins from spots with significantly altered volumes

2D spot No.	Gene bank Accession No.	Gene Name	Sequence Coverage (%)	Unique peptide detected	Predicted M.W. (kDa)	Predicted pI (pH)
302	AAN09299.1	Heat shock protein	30.48	12	72.27	4.99
		cognate 3	6.71	3	71.83	7.07
		(HSC3)				
	AAF48831.1	Transferrin 1 (Tsf1)				
306	AAN09299.1	HSC 3	22.26	10	72.27	4.99
309	AAN09299.1	Heat shock protein	18.60	7	72.27	4.99
		cognate 3	4.52	2	71.83	7.07
	AAF48831.1	Tsf 1				
640	AAF49476.1	Cuticular protein 72Ec	11.19	3	50.58	5.15
775	AAN11026.1	lethal (2) 37Cc	25.72	5	28.3	5.80
853	EAA46049.1	Sarcoplasmic calcium-binding protein 1	39.68	5	21.65	4.50
1783	AAN11962.1	Heat shock protein 22	25.28	3	19.77	4.95
		(HSP22)				

altered susceptibilities to oxidative and/or ER stress. Previous studies have shown that the susceptibility of flies to oxidative stress can be determined by treating them with H₂O₂ or paraquat [38]. When flies were reared on foods containing 1% H₂O₂, the HTorA^{ΔE}-expressing flies exhibited significantly more susceptibility to H₂O₂-induced oxidative stress than the HTorA^{WT}-expressing flies (Figure 4A). The hazard ratio (HR) of the HTorA^{ΔE}-expressing flies was 2.073 compared with the HTorA^{WT}-expressing flies. In addition, the HR of the HTorA^{ΔE}-expressing flies was 3.564 compared with the HTorA^{WT}-expressing flies when exposed to 20 mM paraquat (Figure 4B).

The HR of the HTorA^{ΔE}-expressing flies to tunicamycin induced ER stress was 3.013 compared with the HTorA^{WT}-expressing flies (Figure 4C). However, there was no difference in dithiothreitol (DTT) sensitivity between the HTorA^{WT}- and the HTorA^{ΔE}-expressing flies when the flies were treated with 5 mM, 25 mM or 100 mM DTT (Figure 4D-F). Because tunicamycin and DTT have been known to activate UPR signalling by a different mechanism, these results suggest that HTorA^{ΔE} may induce the activation of specific pathways in the UPR.

HTorA^{ΔE}-expressing flies showed increased sensitivities to autophagy inhibitors

In a previous study, we showed that protein aggregates induced by HTorA^{ΔE} localised to the nuclear membrane, mitochondria, synapses, single membrane lysosomes and double membrane autophagosomes [29]. Because mutations that are known to cause defects in autophagy are related to various neurological disorders [11,48], we further investigated whether HTorA^{ΔE} flies showed altered sensitivities to 3 different autophagy inhibitors (Figure 4

G, H, and I). These results suggested that formations of autophagosomes in HTorA^{ΔE} flies may be involved in protecting flies from HTorA^{ΔE} induced toxicities.

Altered transcript levels of Atf6, Calreticulin, *Drosophila* glucose regulated protein 170 (dGRP170), Activating transcription factor 4 (Atf4), and components of the ERAD pathway in the HTorA^{ΔE}-expressing brains

To further investigate the molecular and cellular mechanisms underlying UPR activation in the HTorA^{ΔE}-expressing brains, the levels of transcripts of three UPR inducers and ER-stress (ERSE) and UPR target genes (UPRE) [7,49] were quantified and compared with those of the HTorA^{WT}-expressing brains by performing qRT-PCR (Additional files 1 and 2). Of the three UPR inducers, the transcript level of Atf6 was significantly increased in the HTorA^{ΔE}-expressing flies (Figure 5A). The expression of the stress-responsive activating transcription factor-4 (Atf4), a downstream regulator of the UPR genes that is activated by *Drosophila* PERK (PEK), was significantly increased (Figure 5A). In addition, the transcription levels of Calreticulin, ERp60, PDI, *Drosophila* homologue of GRP170 (dGRP170), and P58IPK were significantly different, whereas those of Calnexin 99A, GP93 (*Drosophila* homologue of GRP94), and *Drosophila* homologue of Sil1 (dSil1) were the same between the two fly groups (Figure 5A-C). Among the ERAD components tested, the transcripts of Hrd1, Hrd3, Derlin-1, EDEM1, and EDEM2 were also significantly different (Figure 5C).

Because the HTorA^{ΔE} flies showed significantly increased susceptibilities to autophagy inhibitors (Figure 4 G-4I), we also examined any change in the expression of autophagy-related genes (Atgs) in the HTorA^{ΔE} flies. Among 13 Atgs tested, only Atg8b was found to have a

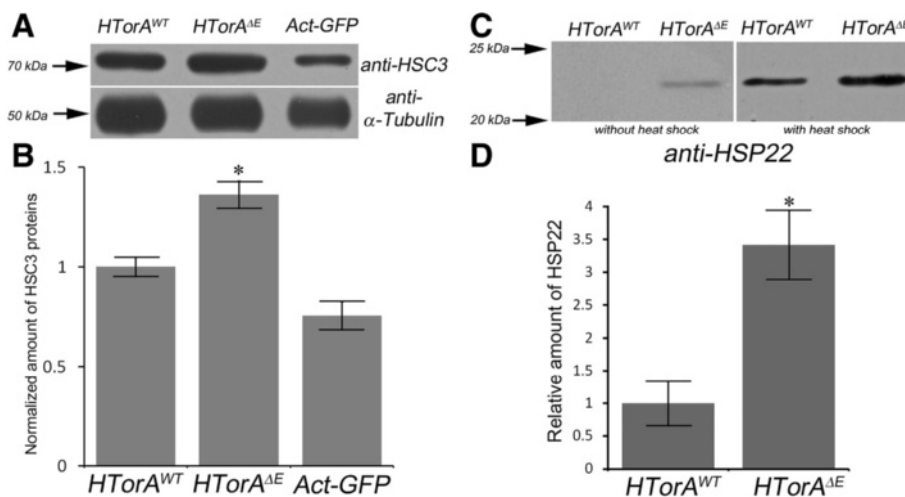


Figure 2 The *HTorA^{AE}*-expressing flies had significantly increased HSC3 and HSP22 in their brains. **(A and B)** When the amounts of HSC3 were normalised with α -Tubulin as a loading control, the *HTorA^{AE}*-expressing brains had 1.4-fold more HSC3 than those of the *HTorA^{WT}*-expressing brains. However, Actin-enhanced Green fluorescence protein (Act-eGFP) expressing flies showed similar expression levels of HSC3. **(C and D)** In normal condition, HSP22 was detected from only the crude mitochondrial fraction of the *HTorA^{AE}*-expressing brains and it was 3.4-fold more abundant in the crude mitochondrial fraction of the *HTorA^{AE}*-expressing brains than that of the *HTorA^{WT}*-expressing brains before or following a heat shock. * = $p < 0.05$.

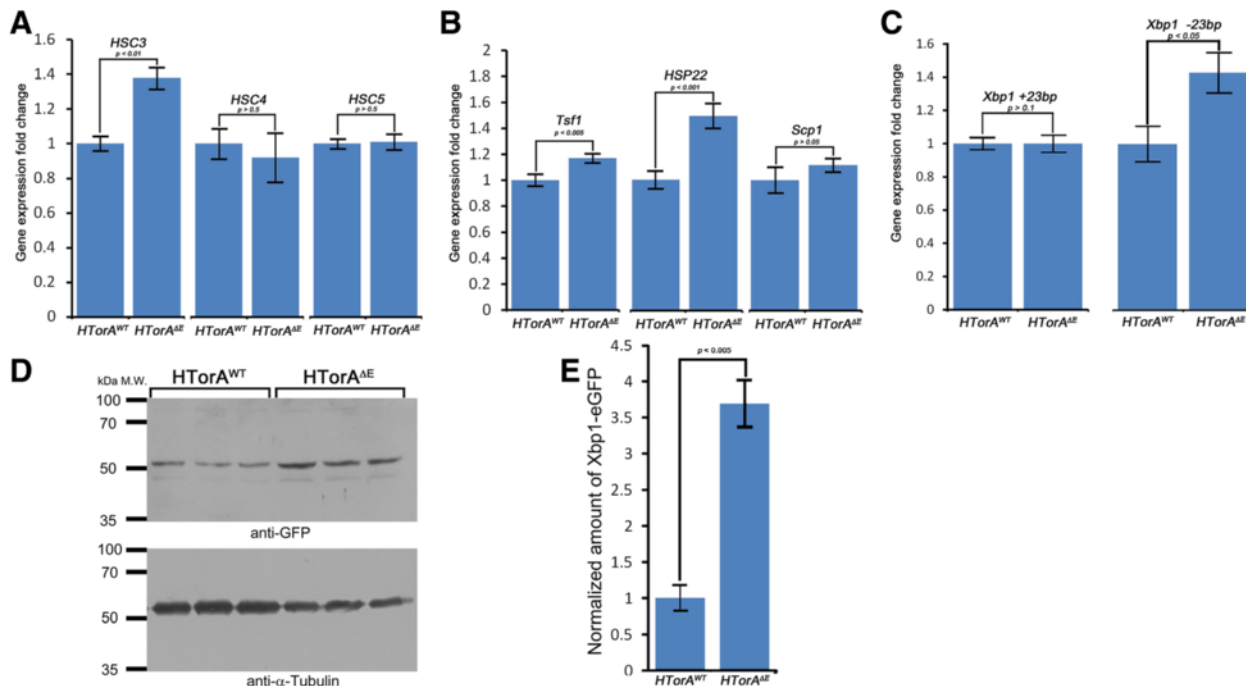
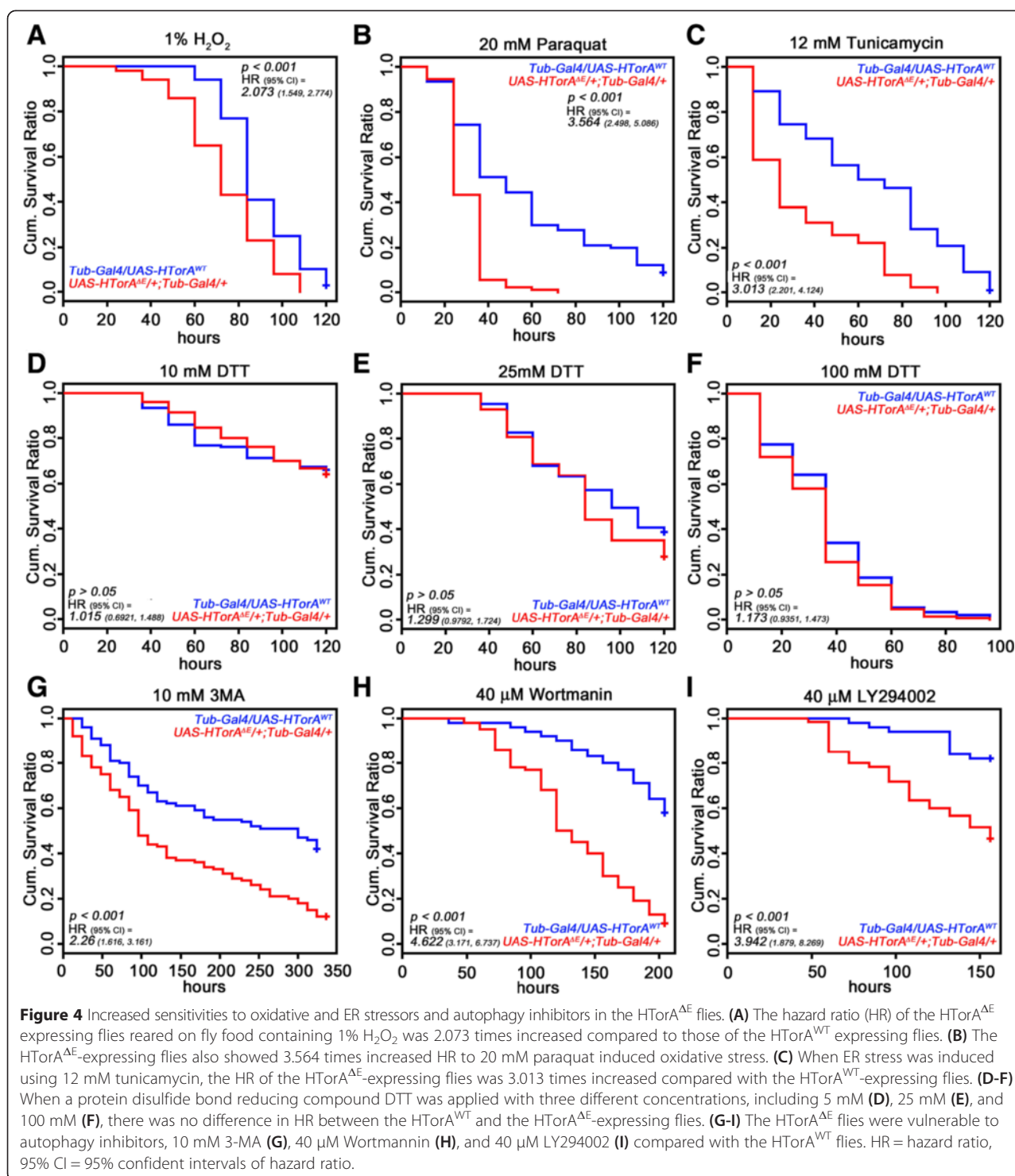
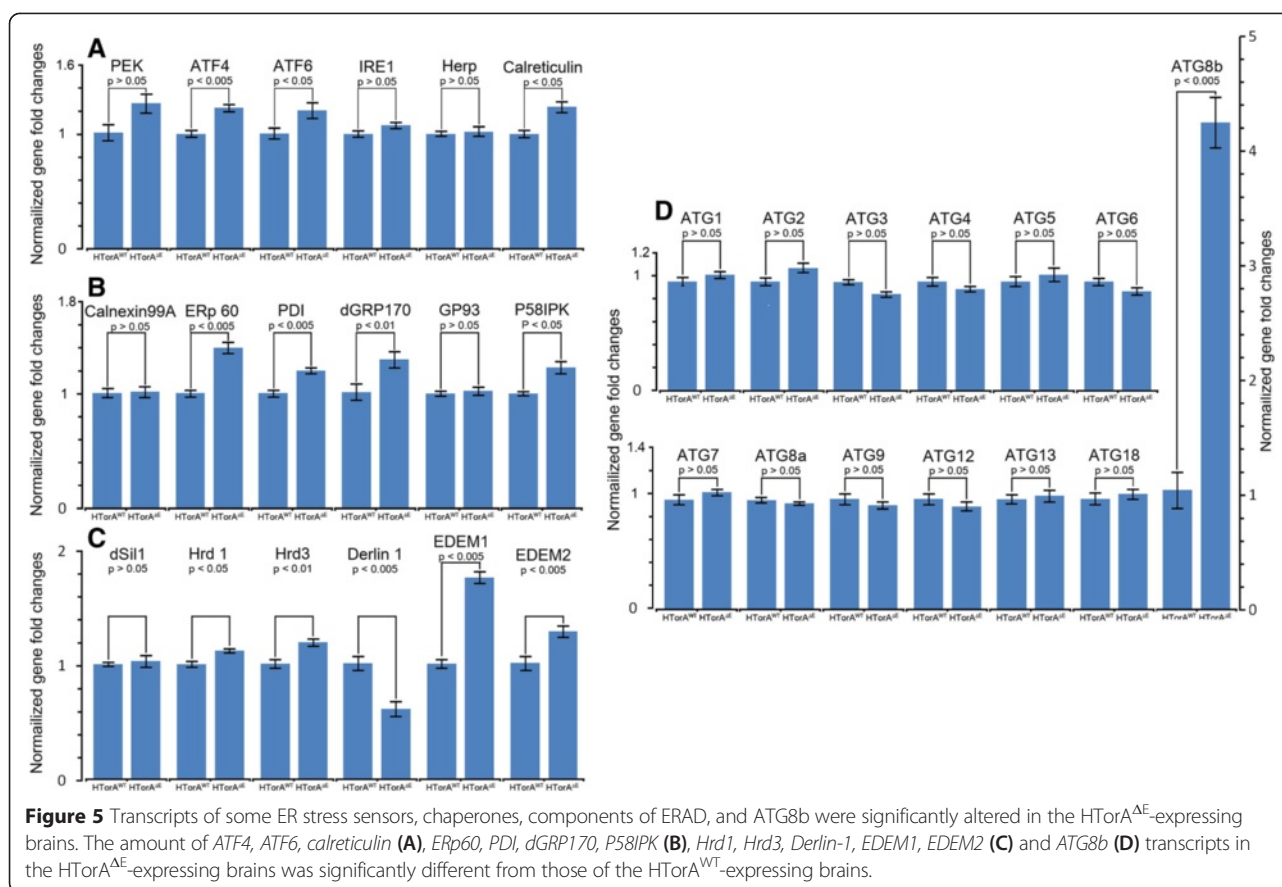


Figure 3 Transcripts of HSC3, HSP22, Tsf1 and IRE1-dependent spliced Xbp1 and Xbp1-eGFP signals were significantly increased in the *HTorA^{AE}*-expressing brains. Quantitative-RT-PCR results of genes encoding proteins displaying the largest alterations in expression in the 2-DE analysis. **(A)** Only the transcripts of *heat shock protein cognate 3 (hsc3)* but not those of *hsc4* and *hsc5* were significantly increased in the *HTorA^{AE}* flies. **(B)** The transcripts of *transferrin1 (tsf1)*, *heat shock protein 22 (hsp22)*, and *sarcoplasmic calcium binding protein (scp1)* were not changed. **(C)** The amount of the IRE1-dependent spliced form of Xbp1 mRNA (Xbp1 -23 bp) was increased in the *HTorA^{AE}* brains. **(D)** Compared with *HTorA^{WT}*, expression of *HTorA^{AE}* induced increased expression of Xbp1-eGFP in *Drosophila* heads. α -Tubulin was used as a loading control. **(E)** The normalised amount of the Xbp1-eGFP band in the *HTorA^{AE}* expressing brains was 3.68-fold higher than that in the *HTorA^{WT}*-expressing brains.



significant difference in expression (Figure 5D and E). Taken together, the qRT-PCR results indicated that the three UPR inducers in the ER were activated by HTorA^{ΔE} and that the expression of certain ER chaperones, nucleotide exchange factors, ERAD components and ATG8b was also induced.

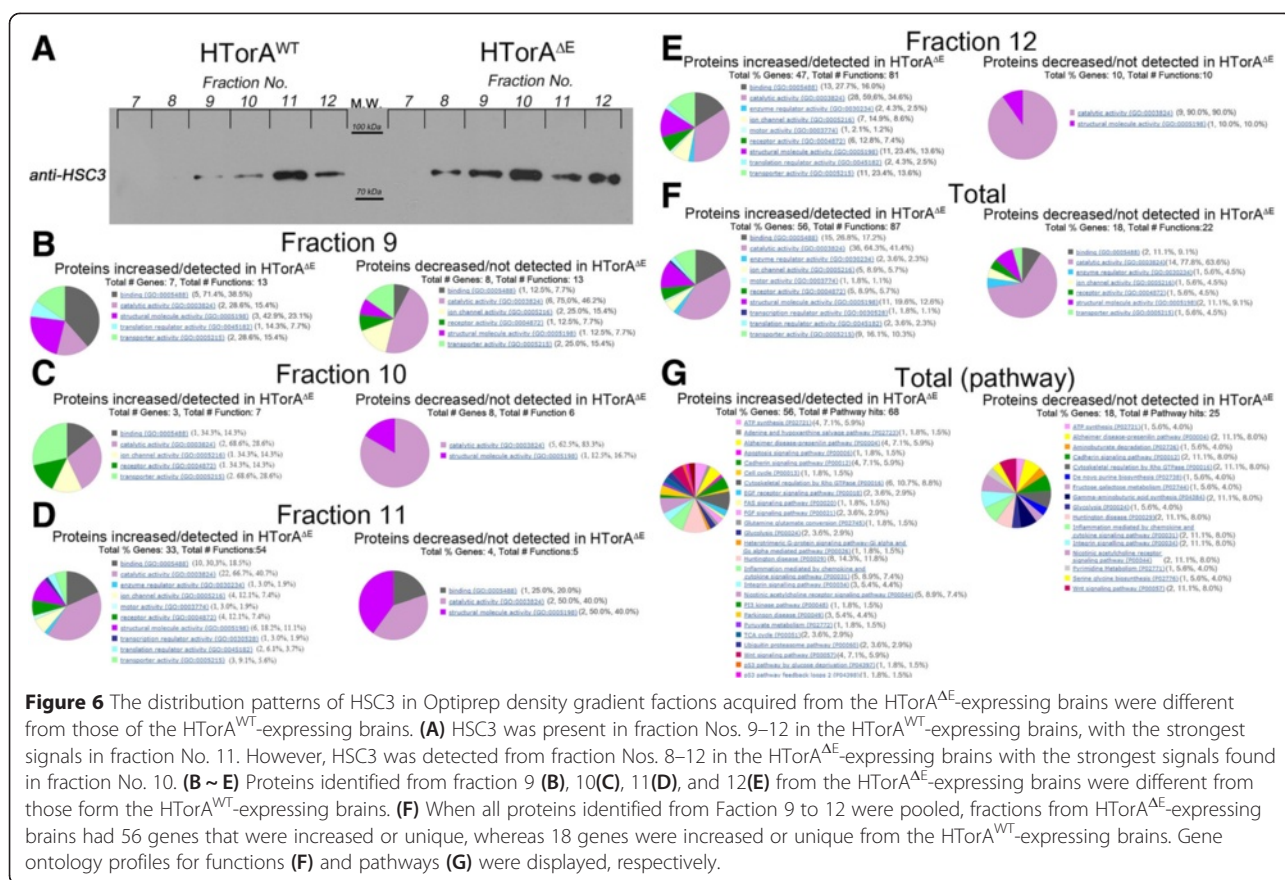
HSC3 positive density gradient fractions of HTorA^{ΔE} and HTorA^{WT} microsomes harboured different protein profiles In addition to their functions as ER stress chaperones [49,50], Bip and its homologues are involved in many molecular chaperone activities in the ER, such as importing newly synthesised proteins across the ER membrane,



increasing the possibility of the correct protein folding, assembly and oligomerisation of the newly synthesised proteins, and controlling Ca²⁺ homeostasis [51,52]. Because several lines of evidence in this study suggested that the HTorA^{ΔE} expression in fly brains may activate the UPR in the ER and perturb ER homeostasis, we reasoned that the biophysical and biochemical properties of the ER in the HTorA^{ΔE} flies might be different than those in the HTorA^{WT} flies. We directly addressed this question by obtaining ER microsomes via density gradient ultra-centrifugation followed by anti-HSC3 western blot analysis and profiling the constituent proteins in those fractions via LC/MS^E proteomic analysis. Interestingly, the fraction Nos. 9–12 obtained from HTorA^{WT} contained HSC3, whereas the fraction Nos. 8–12 from HTorA^{ΔE} were HSC3 positive (Figure 6A). In addition, the fractions that had the most abundant HSC3 immunoreactivity were No. 11 in the HTorA^{WT}-expressing brains versus No. 10 in the HTorA^{ΔE}-expressing brains. Because sedimentation equilibrium density is known to be determined by the sizes, densities, and molecular weights of the proteins comprising macromolecular complexes, differences in the intensities of HSC3 signals in the microsome fractions of the HTorA^{ΔE}- and the HTorA^{WT}-expressing brains suggested that the diversity and quantity of the proteins in the HSC3 positive microsomes might differ from each other.

Indeed, 35 proteins in fractions No. 9, 46 proteins in fractions No. 10, 109 proteins in fractions No. 11, and 160 proteins in fractions No. 12 from the HTorA^{ΔE} and the HTorA^{WT} microsomes were identified using LC/MS^E (Additional file 4). Eight, 4, 41, and 58 proteins in fractions No. 9, 10, 11 and 12, respectively, were increased or detected in the HTorA^{ΔE} microsomes, and 9, 10, 6, and 14 proteins in fractions No. 9, 10, 11 and 12, respectively, were decreased or not detected in the HTorA^{ΔE} microsomes. Greater numbers and types of proteins were present in the HTorA^{ΔE} microsomes than in the HTorA^{WT}, suggesting that HTorA^{ΔE} in the ER may impair the trafficking and secretion of proteins resulting in ER overloads, which is another known ER stressor.

The quantitatively and qualitatively altered proteins in each fraction were divided into groups according to Gene Ontology (GO) molecular functions using Panther version 7 (<http://pantherdb.org>) [53] and AmiGO, the Gene ontology (<http://amigo.geneontology.org/amigo>) [54] (Figure 6 B-G). Of the proteins that were increased or unique to the HTorA^{ΔE}-expressing brains, 71.4% of the annotated proteins in fraction 9 had binding activity (GO:0005488), whereas 68.6%, 66.7% and 59.6% of the annotated proteins in fractions No. 10, 11, and 12, respectively, had catalytic activity (GO:0003824). Other proteins



had structural molecule activity (GO:0005198), translation regulator activity (GO:0045182), transporter activity (GO:0005215), ion channel activity (GO:0005216), receptor activity (GO:0004872), enzyme regulator activity (GO:003234), motor activity (GO:0003774), and transcription regulator activity (GO:0030528) (Figure 6 B-E and Additional file 9). Furthermore, of the proteins that were decreased or not present in the HTorA^{ΔE}-expressing brains, 75.0%, 62.5%, 50.0% and 90.0% of the annotated proteins from fractions No. 9, 10, 11, and 12, respectively, had catalytic activity (GO:0003824). In addition, the proteins with structural molecule activity (GO:0005198) were consistently decreased in all lanes. Other decreased proteins had binding activity (GO:0005488), ion channel activity (GO:0005216), receptor activity (GO:0004872), and transporter activity (GO:0005215) (Figure 6B-E and Additional file 10). When all proteins from fractions No. 9 to 12 were combined for comparison, 68 proteins were increased or unique to HTorA^{ΔE} microsomes. Among 56 annotated proteins, 64.3%, 26.8%, and 19.6% had catalytic activity (GO:0003824), binding activity (GO:0005488) and structural molecule activity (GO:0005198), respectively. Of the 21 proteins decreased or not present in the HTorA^{ΔE} microsomes, 77.8% and 11.1% of the 18 annotated proteins had

catalytic activity (GO:0003824) and binding activity (GO:0005198), respectively (Figure 6F).

The dysregulated proteins in the ER microsomes were further characterised by their association with 165 regulatory and metabolic pathways in the Panther Pathway 3.01 [53]. The following pathways had more than 5 genes associated with them when up-/down-regulated genes were considered simultaneously: the Huntington's disease pathway (P00029), the cytoskeletal regulation by Rho GTPase pathway (P00016), the inflammation mediated by chemokine and cytokine signalling pathway (P00031), the nicotinic acetylcholine receptor signaling pathway (P00044), the Alzheimer's disease-presenilin pathway (P00004), the Cadherin signaling pathway (P00012), the Wnt signaling pathway (P00057) and the ATP synthesis pathway (P02721) (Figure 6 G). These profiling results indicated that HTorA^{ΔE} in the ER involved defects in the synthesis, modification, folding, assembly and trafficking of secretory and membrane proteins that translocate to the cell surface or to intracellular organelles.

Down-regulation of HSC3, Xbp1, ATF6 and Pek in the HTorA^{ΔE} flies induced a significantly earlier death

To understand the physiological consequences of UPR activation in the HTorA^{ΔE} flies, we genetically down-

regulated the expression of *hsc3*, *xbp1*, *ATF6* or *Pek* in the HTorA^{ΔE} flies using RNAi flies for each gene (Additional file 6). When the expression of *hsc3* was down-regulated in the HTorA^{ΔE} flies by RNAi constructs, its HR was 6.579 or 8.135 compared with C155/+; UAS-HTorA^{ΔE}/+ or C155/+; UAS-HSC3-RNAi flies, respectively (Figure 7A and Table 2). We further examined the consequences of the down-regulated expression of *xbp1* by expressing *xbp1*-RNAi constructs or using the *xbp1* mutant chromosome *xbp1*^{K13803} in the HTorA^{ΔE} flies. The down-regulation of *xbp1* expression by *xbp1*-RNAi constructs or mutant chromosome *xbp1*^{K13803} in C155/+; UAS-HTorA^{ΔE}/+ significantly increased the HR to 6.796 or 21.23 compared with C155/+; UAS-HTorA^{ΔE}/+, respectively (Figure 7B and Table 2). The HR of those flies were 5.871 or 15.42 when compared with C155/+; UAS-Xbp1-RNAi or C155/+; *xbp1*^{K13803} flies, respectively (Figure 7B and Table 2). The effect of down-regulation of ATF6 by RNAi in HTorA^{ΔE} flies was less pronounced but also resulted in a significant induction of early death. The HR of C155/+; UAS-HTorA^{ΔE}/UAS-ATF6-RNAi flies were 2.222 and 1.976

compared with C155/+;UAS-HTorA^{ΔE}/+ or C155/+; UAS-ATF6-RNAi/+ flies (Figure 7C and Table 2). In addition, the down-regulation of PEK by *PEK*-RNAi in C155/+;UAS-HTorA^{ΔE} flies induced a significantly earlier death of the flies. The HR of C155/+;UAS-HTorA^{ΔE}/UAS-Pek-RNAi were 2.914 or 7.408 compared with C155/+;UAS-HTorA^{ΔE}/+ or C155/+;UAS-Pek-RNAi (Figure 7D and Table 2).

Discussion

The aim of this study was to elucidate the molecular and cellular consequences of HTorA^{ΔE} in *Drosophila* brains to gain insight into the pathogenesis of DYT1 dystonia. The most interesting finding was that the expression of the ER molecular chaperone HSC3 and a mitochondria specific chaperone HSP22 were significantly increased in the HTorA^{ΔE}-expressing brains obtained from unbiased 2-DE analysis (Figure 1, 2, and Table 1). Those alterations were further verified using western blot and qRT-PCR analyses (Figure 3 and 4).

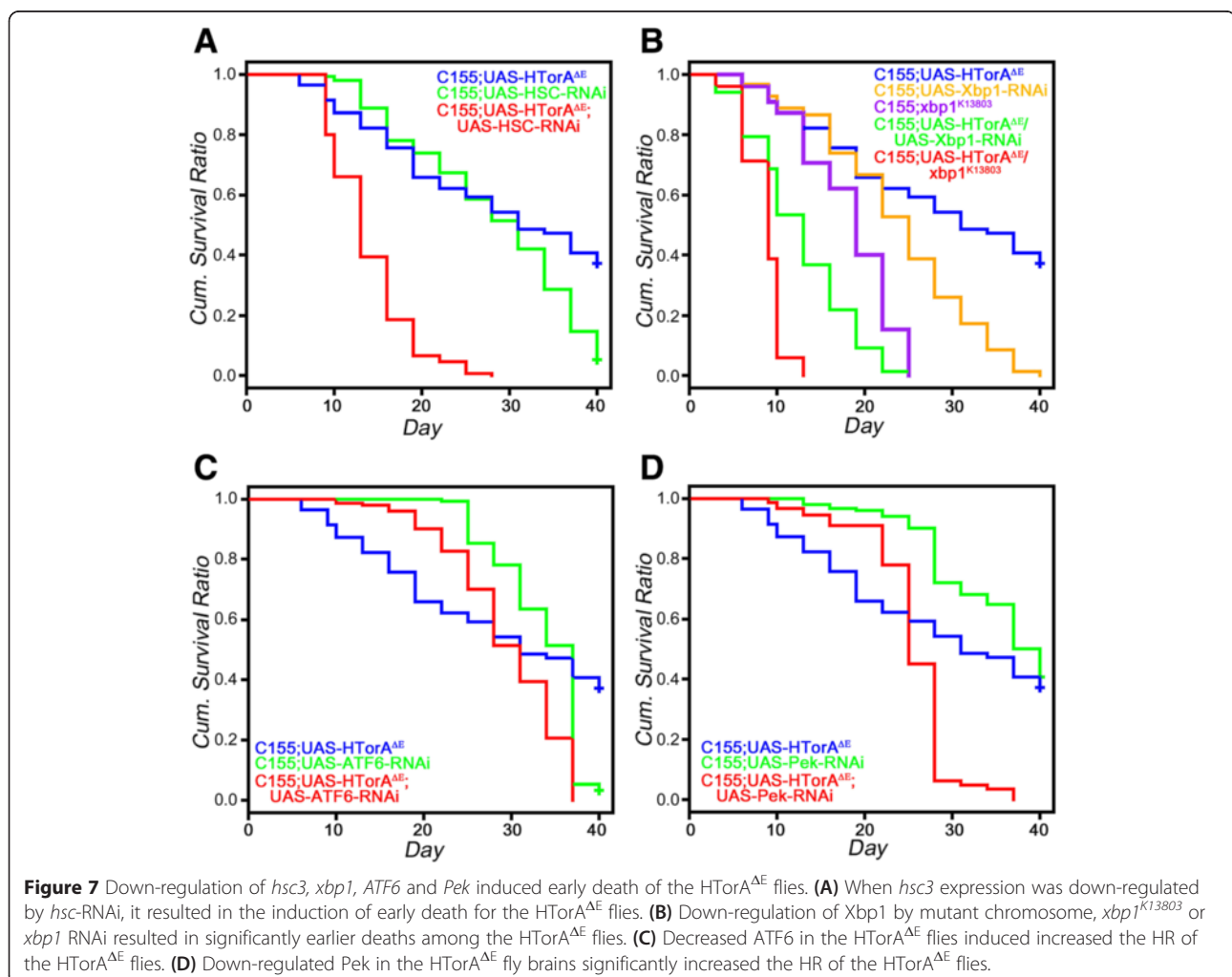


Table 2 The summary of Kaplan-Meier survival analysis with altered expression of UPR sensor and inducers in H₂O₂-expressing flies

Genotype		Trial	p-value ¹	Hazard ratio (95% CI) ²
Control				
A	C155-Gal4/+;UAS-HTor1A ^{ΔE} /+	C155-Gal4/+; UAS-HSC3-RNAi/UAS-HTor1A ^{ΔE}	<0.001	6.579 (4.726, 9.159)
	C155-Gal4/+;UAS-HSC3-RNAi/+		<0.001	8.135 (5.87, 11.27)
B	C155-Gal4/+;UAS-HTor1A ^{ΔE} /+	C155-Gal4/+;UAS-HTor1A ^{ΔE} /UAS-Xbp1-RNAi	<0.001	6.796 (4.865, 9.492)
		C155-Gal4/+;UAS-HTor1A ^{ΔE} /xbp1 ^{K13803}	<0.001	21.23 (13.19, 34.17)
	C155-Gal4/+; UAS-Xbp1-RNAi	C155-Gal4/+;UAS-HTor1A ^{ΔE} /UAS-Xbp1-RNAi	<0.001	5.871 (4.351, 7.924)
	C155-Gal4/+; xbp1 ^{K13803} /+	C155-Gal4/+;UAS-HTor1A ^{ΔE} /xbp1 ^{K13803}	<0.001	15.42 (10.38, 22.9)
C	C155-Gal4/+;UAS-HTor1A ^{ΔE} /+	C155-Gal4/+;UAS-HTor1A ^{ΔE} /UAS-ATF6-RNAi	<0.001	2.222 (1.672, 2.954)
	C155-Gal4/+;UAS-ATF6-RNAi/+		<0.001	1.976 (1.562, 2.499)
D	C155-Gal4/+;UAS-HTor1A ^{ΔE} /+	C155-Gal4/+;UAS-HTor1A ^{ΔE} /UAS-Pek-RNAi	<0.001	2.914 (2.158, 3.934)
	C155-Gal4/+;UAS-Pek-RNAi/+		<0.001	7.408 (5.368, 10.22)

¹p-values were calculated using the log-rank test.

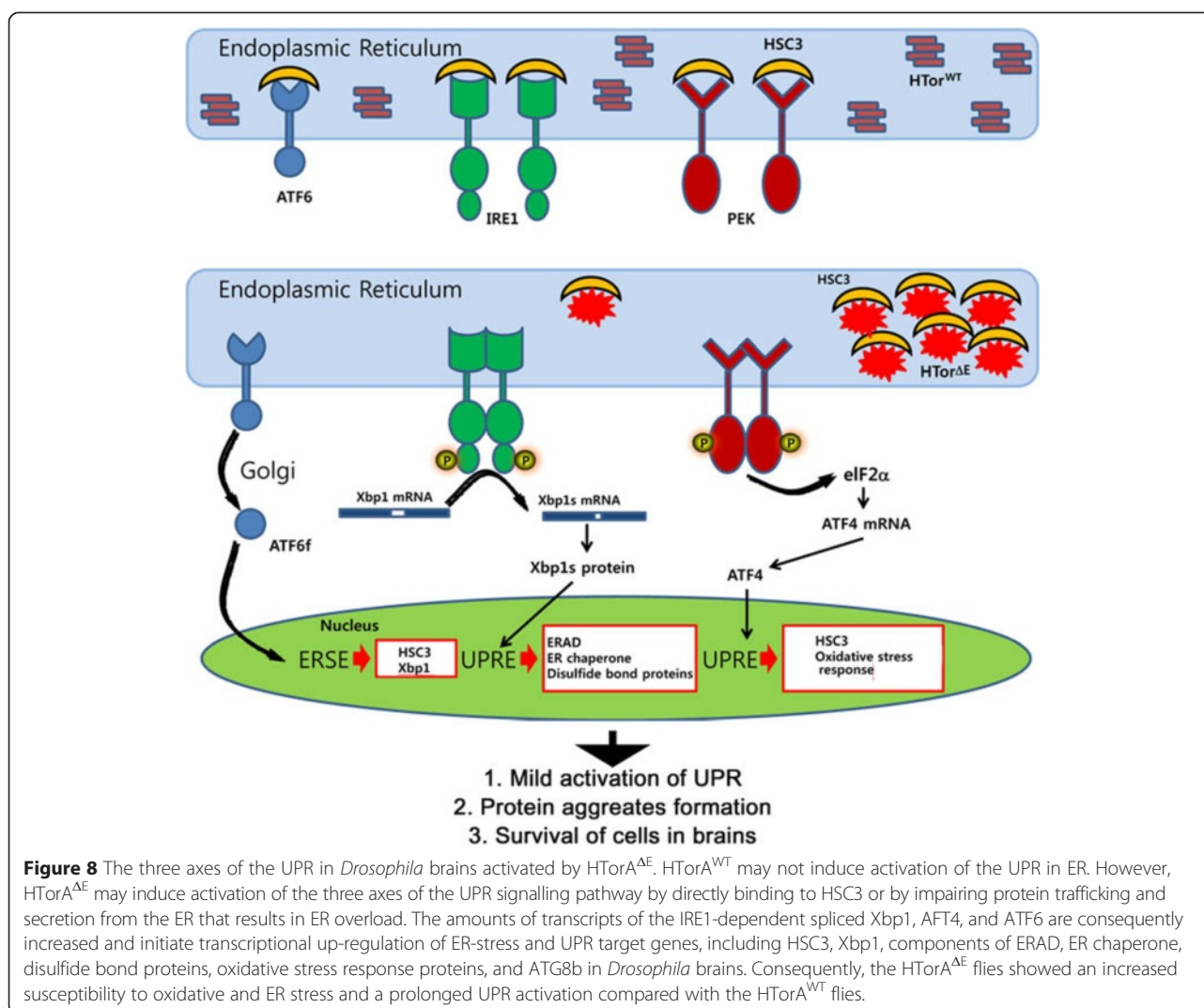
²Hazard ratios and its 95% confidential intervals (CI) were estimated using cox-regression.

Three axes of UPR signaling in the H₂O₂-expressing brains may be activated

The ER chaperone HSC3 (Figure 2 and 3) is a member of the HSP70 protein superfamily and is known to be a *Drosophila* homologue of BiP [8]. Similar to BiP and its homologues in metazoans, HSC3 has been shown to act as an ER stress regulator in flies [8]. For example, the up-regulation of HSC3 upon activation of the UPR has been shown in *Drosophila* models of ADRP [31], congenital glaucoma [47], and Parkinson disease [48]. Similar to those models, we found additional key evidence that UPR activation increased the transcript levels of the IRE1-dependent spliced form of XBP1 (Figure 3C) and the Xbp1-eGFP signal (Figure 3D). Although the amount of IRE1 and PEK mRNAs was not altered, the mRNAs of *ATF6* and *ATF4* were significantly increased in the H₂O₂-expressing brains (Figure 5A). In contrast to the other two UPR inducers that activate downstream transcription factors, Xbp1 and ATF4, ATF6 is transported to Golgi complexes where it is processed into an N-terminal 50 kDa active form that translocates and activates the transcription of the ER stress response genes (ERSE) encoding molecular chaperones and enzymes regulating protein folding and disulfide formation (Figure 8) [5,7]. Thus, the increase of ATF6 transcripts could be interpreted as the activation of the UPR. Further confirmation of UPR activation in H₂O₂-expressing flies was obtained by genetically reducing the expression of UPR sensors and inducers in the H₂O₂-expressing fly brains (Figure 7). The down-regulation of *hsc3*, *xbp1* and *PEK* induced a significantly earlier death in the flies. Although the effects of *ATF6* down-regulation were not as pronounced as those of *hsc3*, *xbp1* and *PEK*, it also induced a significant increase in HR (Figure 7). Taken together, our results suggest that all three UPR inducers may be activated in the H₂O₂-expressing brains.

Increased transcripts of ERSE and UPR in the H₂O₂-expressing brains

One of the enigmatic observations reported from DYT1 dystonia is the absence of obvious pathological lesions in postmortem DYT1 brains [1]. Similarly, the H₂O₂-expressing fly brains do not display any obvious neurodegenerative abnormalities [29,30], suggesting that the presence of the H₂O₂-expressing aggregates in fly brains may not be sufficient to induce apoptosis; however, these aggregates may be sufficient to activate certain adaptive UPR signalling pathways that enable neurons to overcome the toxic effects caused by the accumulation of H₂O₂-expressing in the NE and the ER. Interestingly, we found that the H₂O₂-expressing flies showed some differences in sensitivity to two ER stressors, tunicamycin and DTT (Figure 4). The H₂O₂-expressing were significantly more susceptible to tunicamycin, which inhibits the activity of UDP-N-acetylglucosaminidoliphosphate N-acetylglucosamine-1-phosphate transferase, but not to DTT, which inhibits the formation of disulfide bonds. This observation suggests that other unknown pathways, which were not tested in this study, may exist. In addition, among the ER chaperones, enzymes and nucleotide exchange factors that are known to respond with up-regulation upon activation of the UPR in mammalian cells [7,55], the calreticulin, P58IPK, ERp60, PDI, and dGRP170 transcripts were significantly increased (Figure 5). The increased expression of PDI at the protein level was confirmed by performing protein profiling and semi-quantification analysis in HSC3 positive microsomes (Figure 6, Additional files 4 and 5) and may explain why the H₂O₂-expressing flies did not show DTT sensitivities as PDI activity is important for maintaining DTT resistance in yeast [56]. Thus, H₂O₂-expressing in brains may induce a mild activation of the three branches of the UPR signalling pathway that are sufficient to induce



the expression of some of the ERSE and UPR target genes (UPRE), allowing neurons to overcome and adapt to survival with HTor^{ΔE} (Figure 8).

Degradation of HTor^{ΔE} by ERAD and autophagosome in *Drosophila*

Another known consequence of UPR activation is the degradation of mis-/unfolded proteins by two protein quality control pathways, including ERAD and autophagy [5,8,50]. A recent study in *Drosophila* showed that the over-expression of ERAD components suppressed the onset of retinal degeneration in the *Drosophila* ADRP model by reducing misfolded, mutated Rh-1 proteins [57]. Thus, the increased transcription levels of components of the ERAD (Figure 5C) in the HTor^{ΔE} fly brains suggest that misfolded HTor^{ΔE} might be metabolised by the ERAD pathway. These misfolded proteins may be exported from the ER and degraded by proteasomes in the cytosol. Interestingly, a recent study

using a DYT1 neuronal cell line model demonstrated that HTor^{ΔE} was degraded by both the proteasome and the macroautophagy-lysosome pathway and that HTor^{WT} was mainly degraded by the macroautophagy-lysosome pathway [58]. We also provided several lines of evidence suggesting the involvement of autophagy in HTor^{ΔE} degradation. First, we observed increased transcription levels of ATG8b, which shares 82% amino acid sequence identity and 94% similarity with ATG8a, another *Drosophila* homologue of LC3s [59]. The overexpression of ATG8a has been shown to extend the life span and resistance to oxidative stress in flies [59]. However, the consequences of ATG8b loss or gain of function mutations remain unknown. Nevertheless, both the 4.4-fold increase of ATG8b transcription levels present in the HTor^{ΔE} brains (Figure 5E) and the increased susceptibility to autophagy inhibitors in the HTor^{ΔE} flies (Figure 4 G-I) suggest that autophagosomes may be increased in the HTor^{ΔE} brains and play a pivotal role

in the metabolism of HTorA^{ΔE}. Furthermore, in a previous study, we showed that the HTorA^{ΔE} aggregates in flies are colocalised with a lysosome marker and present within the double membrane structures at EM levels that are similar to autophago-lysosomes [29].

HSP22, sensitivity to oxidative stress and the proteins involved in ATP synthesis, glycolysis and the TCA cycles were altered in the microsomes of HTorA^{ΔE} flies

Drosophila HSP22 is a small heat shock chaperone known to be involved in the regulation of cell proliferation and carcinogenesis [60]. In addition, HSP22 has been shown to be induced in response to acute heat and oxidative stress and is increased with normal aging in flies [36,46]. The over-expression of HSP22 in flies was sufficient to increase resistance to oxidative stress and extend life span [36]. Thus, transcriptional and translational increases of HSP22 in the HTorA^{ΔE}-expressing brains (Figure 2 and 3) may be one of the molecular consequences for overcoming HTorA^{ΔE}-induced defects that might be similar to the defects induced by acute heat and oxidative stress to brains. Considering this observation together with the activation of the UPR may help to explain why the HTorA^{ΔE}-expressing flies had similar life spans to those of the HTorA^{WT}-expressing flies and why they did not manifest severe dystonic symptoms under normal conditions despite the presence of protein aggregates at the NE, the ER and the mitochondria and structural defects at the synapses [29,30]. The increased HSP22 in the HTorA^{ΔE} flies might compensate for those defects caused by the presence of HTorA^{ΔE} under normal conditions. However, if the HTorA^{ΔE} flies were exposed to additional environmental stressors that usually do not induce severe defects in the HTorA^{WT} flies because of the protections afforded by HSP22 induction, the HTorA^{ΔE} flies would be susceptible to those stresses because HSP22 is no longer protecting the neurons and the brains. Indeed, we presented additional evidence to support this notion, such as the increased oxidative stress sensitivity of the HTorA^{ΔE}-expressing flies (Figure 4) and the altered levels of proteins associated with ATP synthesis, glycolysis and the TCA cycle in HSC3 positive microsomes (Figure 6 G). In addition, our hypothesis and observation were further supported by recent studies showing that proteins involved in energy metabolism and the redox state were altered in human neuronal cell lines over-expressing HTorA^{ΔE} [27].

Conclusion

In this study, we have provided several lines of evidence that strongly indicate that HtorA^{ΔE} in fly brains may induce prolonged activation of the UPR (Figure 8). Because the expression of HTorA was not induced by treatment of the PC12 cell line [61], the human kidney

cell line [62], or the human glioblastoma cell line [63] with ER stressors, it may not belong to the group of ER chaperones that are up-regulated upon UPR activation. Moreover, recent studies utilising fibroblasts from DYT1 dystonia patients [17,18] suggest that HTorA is an ER molecular chaperone that regulates the trafficking and secretion of membranes and/or secretory proteins. The fact that treatment with tunicamycin was enough to induce the UPR activation but that neither HTorA^{WT} nor HTorA^{ΔE}-expression in a human glioblastoma cell line did so [62,63] suggested that the expression of HTorA^{ΔE} may not be sufficient for the activation of the UPR in this tumor cell line system. How can we explain the discrepancy between our results and those reported from the DYT1 cellular models? A wide variety of tumours, such as glioblastomas, melanomas, and breast and cervical cancers activate the UPR to allow tumour cells to adapt and survive under certain conditions [4,64,65], and the expression of HTorA^{ΔE} in tumour cell lines may not be sufficient to further induce the activation of the UPR. Similar to our results, the overexpression of HTorA^{ΔE} in *C. elegans* induced the increased expression of its BiP homolog *hsp-4* tagged with GFP and IRE1-dependent spliced Xbp-1 mRNA even before tunicamycin treatment [66]. Furthermore, the decreased export of reporter proteins from DYT1 dystonia fibroblasts compared to those of normal fibroblasts [17,18] could be explained as the activation of the UPR by ER overload because the protein overload is a physiological ER stressor that could initiate UPR activation in the ER [4,49,50]. Thus, it will be intriguing to examine UPR activation and the alteration of HSP22 orthologs in the brains of DYT1 patients and available TG mouse models. Further utilisation of the HTorA^{ΔE}-expressing fly brains will reveal unknown *in vivo* molecular and cellular consequences.

Ethnic statement

We did not use any human subject or data in this study.

Additional files

Additional file 1: The sequences of primers for quantitative real time reverse transcriptase PCR analysis.

Additional file 2: The slope and y intercept of calibration curves and PCR efficiency calculated from slopes for qRT-PCR.

Additional file 3: No differences in survival ratios between HTorAWT- and HTorA^{ΔE}-expressing flies. The p-value calculated using the log-rank test was bigger than 0.1, and the 95% confidential interval of the hazardous ratio was from 0.09092 to 2.699.

Additional file 4: The protein identification results of LC/MSE analysis of HSC3 positive microsome fractions of the HTorA^{ΔE} brains and the HTorAWT brains.

Additional file 5: The label-free semi-quantification results of density gradient fraction Nos. 9–12 from the HTorA^{ΔE} and the HTorAWT brains.

Additional file 6: Transgenic expression of RNAi constructs for hsc3, xbp1, PEK, and ATF6 significantly reduced the amounts of their target mRNAs in fly brains.

Additional file 7: Proteins identified from differentially expressed spots by a nano-HPLC ESI-quadrupole IT MS.

Additional file 8: Expression of Drosophila Torsin proteins did not change expression levels of HSC3. A) Western blot analysis results with rat anti-HSC3, mouse anti- α -Tubulin, and rabbit anti-DTor antibodies. B) Normalized amounts of HSC3 in DTor overexpressing flies were similar to the levels of control flies (Tub-Gal4/+). C) Normalized amounts of DTor in DTor overexpressing flies were 3.5-fold up-regulated compared to the levels of control flies (Tub-Gal4/+). * = $p < 0.05$.

Additional file 9: The list of proteins with increased amounts in density gradient fraction No. 9–12 from the HTorA^{ΔE} and the HTorA^{WT}-expressing brains.

Additional file 10: The list of proteins with decreased amounts in density gradient fraction No. 9–12 from the HTorA^{ΔE} and the HTorA^{WT}-expressing brains.

Abbreviations

2-DE: Two-dimensional electrophoresis; AAA+ ATPase: ATPases associated with a variety of cellular activities; Act-eGFP: Actin-enhanced green fluorescence protein; ADRP: Autosomal dominant retinitis pigmentosa; ATF6: Activating transcription factor 6; Cpr72: Cuticular protein 72Ec; DTT: Dithiothreitol; ΔE: A glutamic deletion; eGFP: Enhanced green fluorescence protein; ER: Endoplasmic reticulum; ERAD: ER associated degradation; ERSE: Endoplasmic reticulum stress response element; GRP78: Glucose-regulated protein 78; HR: Hazard ratio; HSC3: Heat shock cognate 3; HSP22: Heat shock protein 22; HSPA5: Heat shock 70 kDa protein 5; HTorA: Human Torsin A; IRE1: Inositol-requiring enzyme 1; KLC1: Kinesin light chain 1; LAP1: Lamina-associated polypeptide 1; LC: Liquid chromatography; LULL1: Luminal domain like LAP1; MS: Mass spectrometry; NE: Nuclear envelope; PEK: Pancreatic eIF-2 α kinase; PERK: Pancreatic ER kinase; QRT: Quantitative real-time; RIPA: Radio-immuno-precipitation assay; RNAi: inhibitory RNA; SCP1: Sarcoplasmic calcium binding protein 1; SDS: Sodium dodecyl sulfate; si: Small interfering; Tsfl: Transferrin 1; UPLC: Ultra pressure liquid chromatography; UPR: Unfolded protein response; UPRE: Unfolded protein response element; WT: Wild type; xbp1: x-box binding protein 1.

Competing interests

The authors declare that they have no competing interests.

Authors' contributions

AYK, SJB, and KYH designed experiments. AYK, SJB, WTK, HJC, SYK, MG, and YHK performed experiments and data analysis. RT and HS provided materials. RT and HS revised manuscripts. AYK and SJB should be considered as joint first authors. All authors read and approved the final manuscript.

Acknowledgements

This work was carried out with the support of "Cooperative Research Program for Agriculture Science & Technology Development (Project title: Elucidation the health improvement effects of boiled silk worm larvae, Project No:PJ01082801) Rural Development Administration, the Basic Science Research Program through the National Research Foundation of Korea (NRF) funded by the Ministry of Education, Science and Technology (No. 2012R1A1A4A01011674), and KBSI Grant (No. E.34300). HS is an Investigator with the Howard Hughes Medical Institute.

Author details

¹ILSONG Institute of Life Science, Hallym University, 1605-4 Gwanyangdong, Dongan-gu, Anyang, Gyeonggi-do 431-060, Republic of Korea. ²Department of Biomedical Gerontology, Graduate School of Hallym University, Chuncheon, Gangwon-do 200-702, Republic of Korea. ³Korea Basic Science Institute, Sungbuk-gu, Seoul 136-713, Republic of Korea. ⁴National Academy of Agricultural Science, Rural Development Administration, Suwon 441-707, Republic of Korea. ⁵Department of Molecular Biology, Medical Biochemistry & Pathology, Université Laval, Québec, Qc G1V 0A6, Canada. ⁶Howard Hughes Medical Institute, the Rockefeller University, New York, NY 10065, USA.

Received: 13 September 2014 Accepted: 10 April 2015

Published online: 23 April 2015

References

- McNaught KSP, Kapustin A, Jackson T, Jengelly T-A, JnoBaptiste R, Shashidharan P, et al. Brainstem pathology in DYT1 primary torsion dystonia. *Ann Neurol*. 2004;56(4):540–7.
- Ross CA, Poirier MA. Protein aggregation and neurodegenerative disease. *Nat Med*. 2004;10:S10–7.
- Peter OB, Nobuyuki N. The pathogenic mechanisms of polyglutamine diseases and current therapeutic strategies. *J Neurochem*. 2009;110(6):1737–65.
- Lin JH, Walter P, Yen TSB. Endoplasmic reticulum stress in disease pathogenesis. *Annu Rev Pathol*. 2008;3(1):399–425.
- Scheper W, Hoozemans JJM. Endoplasmic reticulum protein quality control in neurodegenerative disease: the good, the bad and the therapy. *Curr Med Chem*. 2009;16:615–26.
- Kim I, Xu W, Reed JC. Cell death and endoplasmic reticulum stress: disease relevance and therapeutic opportunities. *Nat Rev Drug Discov*. 2008;7(12):1013–30.
- Dudek J, Benedix J, Cappel S, Greiner M, Jalal C, Müller L, et al. Functions and pathologies of BiP and its interaction partners. *Cell Mol Life Sci*. 2009;66(5):1556–69.
- Rasheva V, Domingos P. Cellular responses to endoplasmic reticulum stress and apoptosis. *Apoptosis*. 2009;14(8):996–1007.
- Mendes CS, Leviet C, Chatelain G, Dourlen P, Fouillet A, Dichtel-Danjoy M-L, et al. ER stress protects from retinal degeneration. *EMBO J*. 2009;28(9):1296–307.
- Hoozemans JJM, van Haastert ES, Nijholt DAT, Rozemuller AJM, Eikelenboom P, Scheper W. The unfolded protein response is activated in pretangle neurons in Alzheimer's disease hippocampus. *Am J Pathol*. 2009;174(4):1241–51.
- Chu CT. A pivotal role for PINK1 and autophagy in mitochondrial quality control: implications for Parkinson disease. *Hum Mol Genet*. 2010;19(R1):R28–37.
- Hetz C, Thielen P, Matus S, Nassif M, Court F, Kiffin R, et al. XBP-1 deficiency in the nervous system protects against amyotrophic lateral sclerosis by increasing autophagy. *Genes Dev*. 2009;23(19):2294–306.
- Ozelius LJ, Hewett JW, Page CE, Bressman SB, Kramer PL, Shalish C, et al. The early-onset torsion dystonia gene (DYT1) encodes an ATP-binding protein. *Nat Genet*. 1997;17(1):40–8.
- Risch NJ, Bressman SB, Senthil G, Ozelius LJ. Intragenic Cis and Trans modification of genetic susceptibility in DYT1 torsion dystonia. *Am J Hum Genet*. 2007;80:1188–93.
- Granata A, Schiavo G, Warner TT. TorsinA and dystonia: from nuclear envelope to synapse. *J Neurochem*. 2009;109(6):1596–609.
- Neuwald AF, Aravind L, Spouge JL, Koonin EV. AAA+: A class of chaperone-like ATPases associated with the assembly, operation, and disassembly of protein complexes. *Genome Res*. 1999;9(1):27–43.
- Hewett JW, Tannous B, Niland BP, Nery FC, Zeng J, Li Y, et al. Mutant torsinA interferes with protein processing through the secretory pathway in DYT1 dystonia cells. *Proc Natl Acad Sci USA*. 2007;104(17):7271–6.
- Hewett JW, Nery FC, Niland B, Ge P, Tan P, Hadwiger P, et al. siRNA knock-down of mutant torsinA restores processing through secretory pathway in DYT1 dystonia cells. *Hum Mol Genet*. 2008;17(10):1436–45.
- Goodchild RE, Dauer WT. Mislocalization to the nuclear envelope: an effect of the dystonia-causing torsinA mutation. *Proc Natl Acad Sci USA*. 2004;101(3):847–52.
- Dang MT, Yokoi F, McNaught KSP, Jengelly T-A, Jackson T, Li J, et al. Generation and characterization of Dyt1 ΔGAG knock-in mouse as a model for early-onset dystonia. *Exp Neurol*. 2005;196(2):452–63.
- Shashidharan P, Sandu D, Potla U, Armata IA, Walker RH, McNaught KS, et al. Transgenic mouse model of early-onset DYT1 dystonia. *Hum Mol Genet*. 2005;14(1):125–33.
- Goodchild RE, Dauer WT. The AAA+ protein torsinA interacts with a conserved domain present in LAP1 and a novel ER protein. *J Cell Biol*. 2005;168(6):855–62.
- Naismith TV, Dalal S, Hanson PI. Interaction of TorsinA with its major binding partners is impaired by the dystonia-associated ΔGAG deletion. *J Biol Chem*. 2009;284(41):27866–74.
- Hewett JW, Zeng J, Niland BP, Bragg DC, Breakefield XO. Dystonia-causing mutant torsinA inhibits cell adhesion and neurite extension through interference with cytoskeletal dynamics. *Neurobiol Dis*. 2006;22(1):98–111.

25. Kamm C, Boston H, Hewett J, Wilbur J, Corey DP, Hanson PJ, et al. The early onset dystonia protein TorsinA interacts with Kinesin light chain 1. *J Biol Chem*. 2004;279(19):19882–92.
26. Kim CE, Perez A, Perkins G, Ellisman MH, Dauer WT. A molecular mechanism underlying the neural-specific defect in torsinA mutant mice. *Proc Natl Acad Sci USA*. 2010;107:9861–6.
27. Martin JN, Bair TB, Bode N, Dauer WT, Gonzalez-Alegre P. Transcriptional and proteomic profiling in a cellular model of DYT1 dystonia. *Neuroscience*. 2009;164(2):563–72.
28. Walter M, Bonin M, Pullman RS, Valente EM, Loi M, Gambarin M, et al. Expression profiling in peripheral blood reveals signature for penetrance in DYT1 dystonia. *Neurobiol Dis*. 2010;38:192–200.
29. Koh Y-H, Rehfeld K, Ganetzky B. A *Drosophila* model of early onset torsion dystonia suggests impairment in TGF- β signaling. *Hum Mol Genet*. 2004;13(18):2019–30.
30. Lee DW, Seo JB, Ganetzky B, Koh YH. Δ FY mutation in human torsin A induces locomotor disability and aberrant synaptic structures in *Drosophila*. *Mol Cells*. 2009;27(1):89–97.
31. Ryoo HD, Domingos PM, Kang M-J, Steller H. Unfolded protein response in a *Drosophila* model for retinal degeneration. *EMBO J*. 2007;26(1):242–52.
32. Lee D-W, Seo JB, Nam MH, Kang JS, Kim SY, Kim AY, et al. A combination of biochemical and proteomic analyses reveals Bx-LEC-1 as an antigenic target for the monoclonal antibody 3-2A7-2H5-D9-F10 specific to the pine wood nematode. *Mol Cell Proteomics*. 2011;10:M900521–MCP200.
33. Park Y, Kim W, Kim AY, Choi HJ, Choi JK, Park N, et al. Normal prion protein in *Drosophila* enhances the toxicity of pathogenic polyglutamine proteins and alters susceptibility to oxidative and autophagy signaling modulators. *Biochem Biophys Res Commun*. 2011;404(2):638–45.
34. Morrow G, Inaguma Y, Kato K, Tanguay RM. The small heat shock protein Hsp22 of *Drosophila melanogaster* is a mitochondrial protein displaying oligomeric organization. *J Biol Chem*. 2000;275(40):31204–10.
35. Miwa S, St-Pierre J, Partridge L, Brand MD. Superoxide and hydrogen peroxide production by *Drosophila* mitochondria. *Free Radic Biol Med*. 2003;35(8):938–48.
36. Morrow G, Samson M, Michaud S, Tanguay RM. Overexpression of the small mitochondrial Hsp22 extends *Drosophila* life span and increases resistance to oxidative stress. *FASEB J*. 2014;18:598–9.
37. Bustin SA, Benes V, Garson JA, Hellemans J, Huggett J, Kubista M, et al. The MIQE guidelines: minimum information for publication of quantitative real-time PCR experiments. *Clin Chem*. 2009;55(4):611–22.
38. Meulener M, Whitworth AJ, Armstrong-Gold CE, Rizzu P, Heutink P, Wes PD, et al. *Drosophila* DJ-1 mutants are selectively sensitive to environmental toxins associated with Parkinsons disease. *Curr Biol*. 2005;15:1572–7.
39. Xia W, Zhang J, Ostaszewski BL, Kimberly WT, Seubert P, Koo EH, et al. Presenilin 1 regulates the processing of β -amyloid precursor protein C-terminal fragments and the generation of amyloid β -protein in endoplasmic reticulum and golgi. *Biochemistry*. 1998;37(47):16465–71.
40. Tan DJL, Dvinge H, Christoforou A, Bertone P, Martinez Arias A, Lilley KS. Mapping organelle proteins and protein complexes in *drosophila melanogaster*. *J Proteome Res*. 2009;8(6):2667–78.
41. Ono M, Shitashige M, Honda K, Isobe T, Kuwabara H, Matsuzuki H, et al. Label-free quantitative proteomics using large peptide data sets generated by nanoflow liquid chromatography and mass spectrometry. *Mol Cell Proteomics*. 2006;5(7):1338–47.
42. Gao B-B, Stuart L, Feener EP. Label-free quantitative analysis of one-dimensional PAGE LC/MS/MS proteome. *Mol Cell Proteomics*. 2008;7(12):2399–409.
43. Loewen CA, Feany MB. The unfolded protein response protects from Tau Neurotoxicity In Vivo. *PLoS ONE*. 2010;5(9), e13084.
44. Hewett J, Gonzalez-Agosti C, Slater D, Ziefer P, Li S, Bergeron D, et al. Mutant torsinA, responsible for early-onset torsion dystonia, forms membrane inclusions in cultured neural cells. *Hum Mol Genet*. 2000;9(9):1403–13.
45. Kustedjo K, Bracey MH, Cravatt BF. Torsin A and its torsion dystonia-associated mutant forms are luminal glycoproteins that exhibit distinct subcellular localizations. *J Biol Chem*. 2000;275(36):27933–9.
46. Landis GN, Abdueva D, Skvortsov D, Yang J, Rabin BE, Carrick J, et al. Similar gene expression patterns characterize aging and oxidative stress in *Drosophila melanogaster*. *Proc Natl Acad Sci USA*. 2004;101(20):7663–8.
47. Carbone MA, Ayroles JF, Yamamoto A, Morozova TV, West SA, Magwire MM, et al. Overexpression of Myocilin in the *Drosophila* eye activates the unfolded protein response: implications for glaucoma. *PLoS ONE*. 2009;4(1), e4216.
48. Fouillet A, Lvet C, Virgone A, Robin M, Dourlen P, Rieusset J, et al. ER stress inhibits neuronal death by promoting autophagy. *Autophagy*. 2012;8(6):915–26.
49. Todd DJ, Lee A-H, Glimcher LH. The endoplasmic reticulum stress response in immunity and autoimmunity. *Nat Rev Immunol*. 2008;8(9):663–74.
50. Ron D, Walter P. Signal integration in the endoplasmic reticulum unfolded protein response. *Nat Rev Mol Cell Biol*. 2007;8(7):519–29.
51. Marciniak SJ, Ron D. Endoplasmic reticulum stress signaling in disease. *Physiol Rev*. 2006;86(4):1133–49.
52. Hebert DN, Molinari M. In and out of the ER: protein folding, quality control, degradation, and related human diseases. *Physiol Rev*. 2007;87(4):1377–408.
53. Mi H, Dong Q, Muruganujan A, Gaudet P, Lewis S, Thomas PD. PANTHER version 7: improved phylogenetic trees, orthologs and collaboration with the Gene Ontology Consortium. *Nucl Acids Res*. 2010;38(1):D204–210.
54. Carbon S, Ireland A, Mungall CJ, Shu S, Marshall B, Lewis S, et al. AmiGO: online access to ontology and annotation data. *Bioinformatics*. 2009;25(2):288–9.
55. Mendes HF, Cheetham ME. Pharmacological manipulation of gain-of-function and dominant-negative mechanisms in rhodopsin retinitis pigmentosa. *Hum Mol Genet*. 2008;17(19):3043–54.
56. Holst B, Tachibana C, Winther JR. Active site mutations in yeast protein disulfide isomerase cause dithiothreitol sensitivity and a reduced rate of protein folding in the endoplasmic reticulum. *J Cell Biol*. 1997;138(6):1229–38.
57. Kang M-J, Ryoo HD. Suppression of retinal degeneration in *Drosophila* by stimulation of ER-associated degradation. *Proc Natl Acad Sci USA*. 2009;106(40):17043–8.
58. Giles LM, Chen J, Li L, Chin L-S. Dystonia-associated mutations cause premature degradation of torsinA protein and cell-type-specific mislocalization to the nuclear envelope. *Hum Mol Genet*. 2008;17(17):2712–22.
59. Simonsen A, Cumming RC, Brech A, Isakson P, Schubert DR, Finley KD. Promoting basal levels of autophagy in the nervous system enhances longevity and oxidant resistance in adult *Drosophila*. *Autophagy*. 2008;4:176–84.
60. Wadhwa R, Ryu J, Gao R, Choi I-K, Morrow G, Kaur K, et al. Proproliferative functions of *drosophila* small mitochondrial heat shock protein 22 in human cells. *J Biol Chem*. 2010;285(6):3833–9.
61. Hewett J, Ziefer P, Bergeron D, Naismith T, Boston H, Slater D, et al. TorsinA in PC12 cells: Localization in the endoplasmic reticulum and response to stress. *J Neurosci Res*. 2003;72(2):158–68.
62. Bragg DC, Camp SM, Kaufman CA, Wilbur JD, Boston H, Schuback DE, et al. Perinuclear biogenesis of mutant torsin-a inclusions in cultured cells infected with tetracycline-regulated herpes simplex virus type 1 amplicon vectors. *Neuroscience*. 2004;125(3):651–61.
63. Bragg DC, Kaufman CA, Kock N, Breakefield XO. Inhibition of N-linked glycosylation prevents inclusion formation by the dystonia-related mutant form of torsinA. *Mol Cell Neurosci*. 2004;27(4):417–26.
64. Bi M, Naczki C, Koritzinsky M, Fels D, Blais J, Hu N, et al. ER stress-regulated translation increases tolerance to extreme hypoxia and promotes tumor growth. *EMBO J*. 2005;24(19):3470–81.
65. Romero-Ramirez L, Cao H, Nelson D, Hammond E, Lee A-H, Yoshida H, et al. XBP1 is essential for survival under hypoxic conditions and is required for tumor growth. *Cancer Res*. 2004;64(17):5943–7.
66. Chen P, Burdette AJ, Porter JC, Ricketts JC, Fox SA, Nery FC, et al. The early-onset torsion dystonia-associated protein, torsinA, is a homeostatic regulator of endoplasmic reticulum stress response. *Hum Mol Genet*. 2010;19(18):3502–15.

Submit your next manuscript to BioMed Central and take full advantage of:

- Convenient online submission
- Thorough peer review
- No space constraints or color figure charges
- Immediate publication on acceptance
- Inclusion in PubMed, CAS, Scopus and Google Scholar
- Research which is freely available for redistribution

Submit your manuscript at
www.biomedcentral.com/submit

